J Polym Res (2012) 19:9952
DOI 10.1007/s10965-012-9952-z

REVIEW PAPER

Thermo/chemo-responsive shape memory effect in polymers: a sketch of working mechanisms, fundamentals and optimization

W. M. Huang · Y. Zhao · C. C. Wang · Z. Ding · H. Purnawali · C. Tang · J. L. Zhang

Received: 12 May 2012 / Accepted: 30 July 2012 / Published online: 15 August 2012

Abstract Based on the working mechanisms, a systematic literature review is logically presented to reveal that the thermo- and chemo- responsive shape memory effects (SMEs) are not the special phenomena of some particular polymers, but intrinsic features of most polymers (if not all). Subsequently, referring to the most recent experimental results and their theoretical origins, we reveal the fundamentals on the optimization of the SME in polymers and the approaches to design/synthesize polymeric materials with tailored features.

Keywords Shape memory effect · Polymers · Heat · Chemical · Optimization · Mechanisms

Introduction

According to the traditional definition, after being severely and quasi-plastically distorted, shape memory polymers (SMPs), as other shape memory materials (SMMs), are able to recover their original shape at the presence of the right stimulus, such as heat (thermo-responsive), light (photo-responsive), chemical (including water, chemo-responsive) [1–7]. This shape recovery phenomenon is known as the shape memory effect (SME), which provides an alternative approach for many designs that are difficult to achieve using conventional materials/technologies, and thus according to Toensmeier PA [8] reshaping product design. We have seen a variety of applications of SMPs, from surface patterning (e.g., [9–13]) to medical applications [14–18], from space applications [19, 20] to active disassembly [21, 22].

In many occasions in the literature, the SME is discussed together with another shape change phenomenon, i.e., shape change effect (SCE). Different from the SME, in which a material is able to virtually keep the quasi-plastic deformation forever, the SCE refers to a kind of elastic or superelastic behavior in response to the right stimulus [7, 23]. For instance, electro-active polymers (EAPs) and polarized piezoelectrical materials (such as lead zirconate titanate, PZT) are able to alter their shape spontaneously when an electrical voltage is applied and return to the original shape instantly upon removal of the voltage. Furthermore, the amount of displacement is about in proportional to the magnitude of the applied voltage [24, 25]. Similarly, we may claim that the elastic deformation in materials is essentially a kind of SCE.

Fundamentally from energy point of view, the difference between SCE and SME is due to the magnitude of energy barrier between two states, in which one is under the right stimulus, and the other is not. As shown in Fig. 1, if the energy barrier between shape *A* and shape *B* is almost zero, upon removal of the applied stimulus, the material is able to return to its original position (the SCE). If the energy barrier is very high (*H*), without additional driving force to overcome the barrier, the material will maintain the deformed shape (the SME). If the barrier is low (*H'*), the material may slowly recover its original position. Viscous-elasticity is a typical example of such. Sometimes, the SME may appear in a gradual manner (typically in responding to light and chemical) due to the nature of time consuming process in accumulating enough driving energy or gradual penetration of the stimulus.

Depending on the exact situation, a material may have the SME or the SCE. Hence, if we classify the exact type of

W. M. Huang (✉) · Y. Zhao · C. C. Wang · Z. Ding · H. Purnawali · C. Tang · J. L. Zhang
School of Mechanical and Aerospace Engineering, Nanyang Technological University,
50 Nanyang Avenue,
Singapore, Singapore 639798
e-mail: mwmhuang@ntu.edu.sg

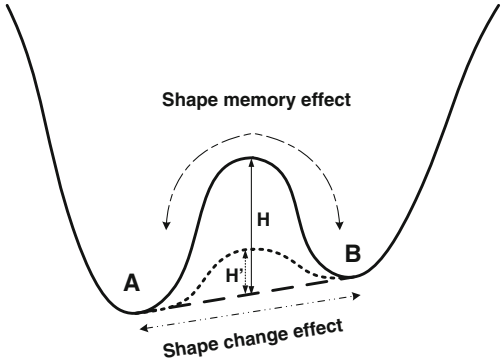

Fig. 1 Shape memory effect (SME) and shape change effect (SCE)

material according to the composition/molecular structure, a material may belong to both SMM and shape change material (SCM). For example, at low temperatures, a shape memory alloy (SMA) has the SME (and thus, belongs to the family of SMM); on the other hand, at high temperatures, it behaves superelastically in responding to mechanical loading, and hence is the SCE [26, 27]. SMPs actually share this similarity as SMAs. Consequently, although the focus of this paper is on the SME in polymers, we are not able to totally avoid to mention the SCE.

In recent years, the expansion of the SMP family is rather rapid [7, 28–33]. In addition to the continuous efforts in developing new SMPs and modifying existing ones, excellent SME has been observed in many conventional polymers [22, 34, 35] and even bio-plastics [36]. It should be pointed out that despite heat-shrink polymers and water-shrink polymers have an extremely long history (maybe even well before the term of SME has ever been *coined*), and technically speaking, they should fall into the categories of thermo-responsive SMP and chemo-responsive SMP, respectively, these polymers attract only limited attention from current research community, although there are a range of off-the-shelf products (in particular for packaging) in the current market. Although not so often, here and there in the literature we have seen statement directly or indirectly mentioning that all polymers should have the SME (most likely meant for the thermo-responsive SME, e.g., in a very recent publication by Mendez et al. [37]). Some early experiments conducted on some commonly used engineering polymers (e.g., in [38–51]) have indicated the shape change/recovery phenomenon after annealing. Nevertheless, the exact working mechanisms behind various shape memory features in response to different stimuli and programming methods (i.e., procedures to setup the temporary shape) have yet seemingly to be well established.

Some of the previous efforts aimed to classify SMPs according to their chemical/molecular structures and compositions (e.g., [1, 5, 52]). For instance, Beloshenko et al. [35] proposed four types of thermo-responsive SMPs, namely glassy polymer, crystallisable polymer (further divided into amorphous-crystalline homopolymer and copolymer), polymer blend and filled polymer composite, and polymer gel.

As pointed out by Prof. M Irie in [26], all SMPs fall into three categories according to the nature of stimulus, namely, thermo-responsive SMP, chemo-responsive SMP and photo-responsive SMP. It should be pointed out that almost by default, thermo-responsive is traditionally meant for heating only, even by means of applying many unconventional heating techniques, e.g., inductive heating, joule heating, light heating (within the whole light wavelength range, from ultraviolent to infrared), ultrasonic/acoustic heating etc, which seemingly help to expand the number of SMP categories [53–61]. Cooling for shape recovery is only achieved very recently in a shape memory polymeric hybrid [23]. In order to achieve true "light induced" shape recovery (i.e., without any heat involved), polymers should have a special chemical structure which reacts to light by means of altering the molecular structure [62, 63]. A recently developed polymer which is able to disassemble by means of near infrared irradiation [64] may provide a supplementary approach to traditional triggering methods. Anyway, photo-responsive SME is not a generic feature but limited to only some particular polymers which need to be purposely designed/synthesized in order to have such a function.

In this paper, based on the previous investigations reported in the literature, we summarize the fundamental mechanisms behind the thermo-responsive and chemo-responsive shape recovery phenomena in polymers and polymeric materials according to their working principles. Section "Mechanisms behind thermally induced SME" discusses the basic working mechanisms for the thermally induced SME. Section "Chemically induced SME" is about chemically induced SME. With the mechanisms (from mechanical point of view) in mind, in Section "Fundamentals and optimization of the SME", the fundamentals behind the key aspects of the SME are analyzed in order to achieve optimized performance. Further discussions on some important relevant issues in engineering practice (including multiple-SME, temperature memory effect etc) are presented in Section "Further discussions". Finally, we summarize major conclusions in Section "Conclusions".

We need to bear in mind that although very high recoverable strain is one of the distinguished advantages of SMPs when compared with other SMMs [23, 26, 65, 66], in some engineering applications, a small recoverable strain is preferred. A typical example of such is wrinkling based surface patterning atop polymers [13, 67], in which the required recoverable strain is not more than a few percent. A larger strain may actually cause cracking [68, 69]. A few percent of recoverable strain is actually comparable to the maximum recoverable strain of both copper and NiTi based SMAs in cyclic actuation [65]. On the other hand, full shape recovery may not be a must in all engineering applications, as long as

the amount of recovery can meet the requirements of a particular application. For instance, in packaging industry, the concern is how much a polymer is able to shrink, but not whether the recovery is 100 %.

Mechanisms behind thermally induced SME

For simplification, all time-dependent parameters are ignored. We assume all processes and sub-processes are instantly finished when the specified temperature and stress/strain conditions are reached. Relaxation and creeping, which are commonly observed in viscous materials, particularly in polymers, are not considered.

The heating induced SME in all polymeric materials can be classified into three categories according to their basic working mechanisms as illustrated in Fig. 2.

Dual-state mechanism (DSM)

Within the first category (Type I), assume that a glassy polymer is heated to above its glass transition temperature (T_g) (a) and then deformed in its rubbery state (b). Subsequently, the constraint is removed after it returns to its glassy state (c). Technically speaking, this procedure is often called as "programming" within the SMM community. After programming, the polymer is heated into the rubbery state and the SME can be observed (d). This is actually the category of glassy polymer as mentioned in [35].

In the rubbery state, a polymer is easy to be deformed. Upon cooling into the glassy state, the molecular motion is frozen so that even after the applied constraint is removed, the polymer largely maintains the distorted shape. Shape recovery occurs only when the polymer is heated to the rubbery state again so that the molecular motion is reactivated. We can conclude that by utilizing the glass transition, all elastomers are naturally SMP. Since there are two phases (rubbery and glassy) in this mechanism, we may call it dual-state mechanism (DSM). Among many others, poly(methyl methacrylate) (PMMA) and silicone (Fig. 3) are two typical examples belonging to this category [34, 47].

As pointed out by Xie T [52], good *cross-linked* netpoints (including physical cross-linking, e.g., tangling,

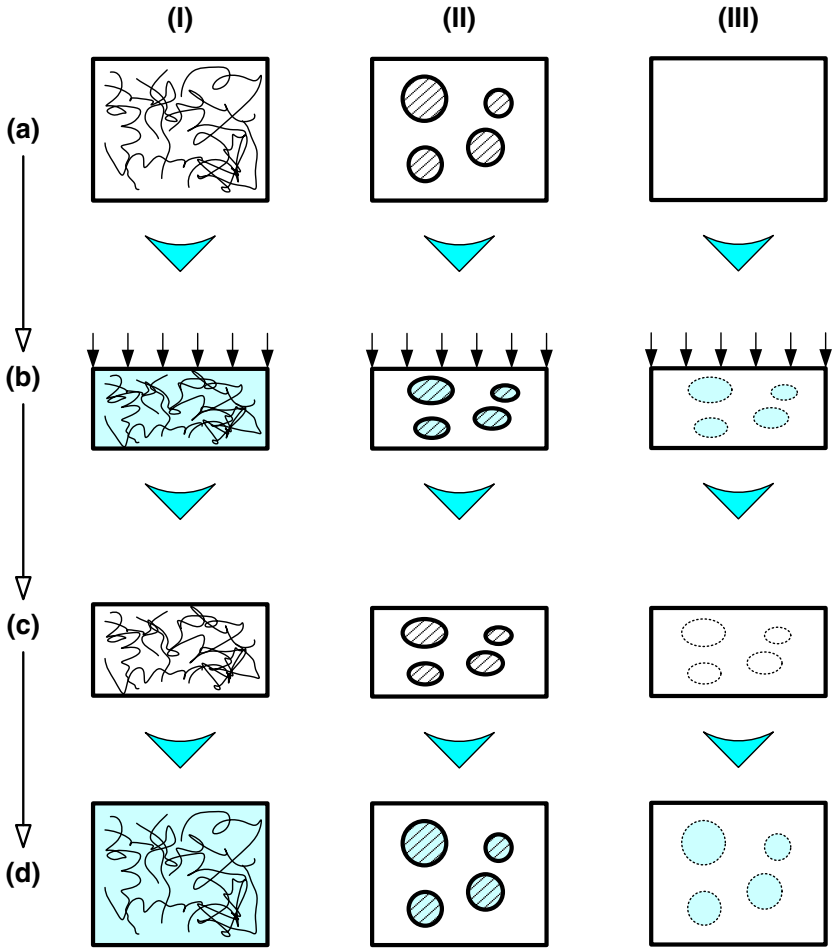

Fig. 2 Basic working mechanisms for the SME in polymeric materials. (I) Dual-state mechanism (DSM); (II) dual-component mechanism (DCM); (III) partial-transition mechanism (PTM). **a** Original sample at room temperature; **b** upon heating and compressing; **c** after cooling and constraint removal; **d** after heating for shape recovery

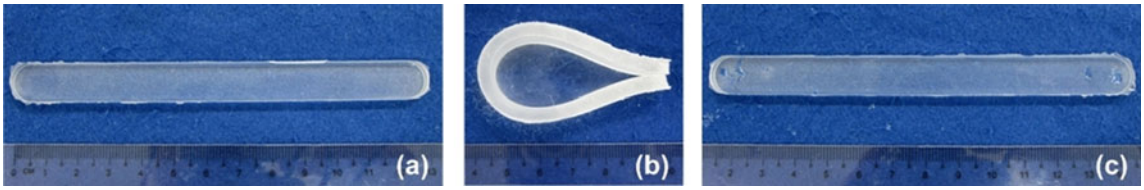

Fig. 3 The SME in silicone. **a** Original shape; **b** cooled in liquid nitrogen (able to maintain this shape in liquid nitrogen as stand-alone); **c** recovered at room temperature

chemical cross-linking, and non-covalent interaction etc [70–73]) is required to ensure a high shape recovery ratio. We may consider that upon cooling to below T_g, the elastic energy in the distorted rubbery polymer is stored as potential energy in the glassy polymer, which provides the driving force for subsequent thermally induced shape recovery.

Dual-component mechanism (DCM)

The SME in ethylene-vinyl acetate (EVA) has been reported many years ago (e.g., in [74]). EVA is a typical copolymer in which one segment is always highly elastic within the whole working temperature range of our interest (elastic segment, which has a relatively higher softening temperature), while the other is able to reversibly change its stiffness from very soft at high temperatures to hard at low temperatures (transition segment, which has a relatively lower softening temperature). After cooling, the EVA, which is expanded during heating to above its transition temperature (the softening temperature of the transition segment), is able to keep the new shape in a larger diameter virtually forever, before being reheated again to fully recover its original size (Fig. 4).

There are many other SMPs which have a similar dual-segment system. A typical example is polyurethane (PU), which might be the SMP that has been subjected to the most intensive investigation (including modification) so far [29, 75–84]. According to Beloshenko et al. [35], these dual-segment polymers belong to the category of crystallisable polymers, which is the second category (II) in Fig. 2.

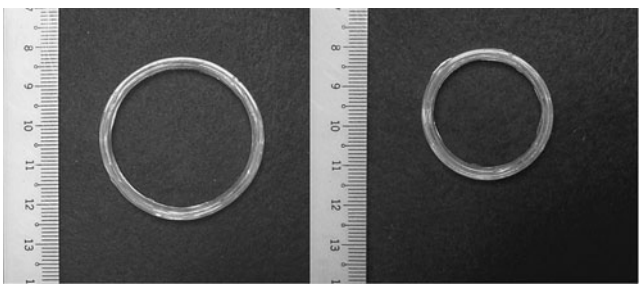

Fig. 4 Thermo-responsive SME in EVA. **a** After expansion; **b** after heating for (full) shape recovery

Materials under Category II are not limited to the ones with a dual-segmented structure, but they include all polymeric materials, which have a dual-component system, i.e., two segments or two domains (illustrated as a matrix/inclusion system in Fig. 2II). Again, one component is always highly elastic (elastic component), while the other (transition component) has a reversible phase transition, which is accompanied by a remarkable change in the stiffness during thermal cycling. The possible phase transition in the transition component might be the glass transition, melting etc, as long as the conditions of reversible and large stiffness change are satisfied.

In [85], the SME has been demonstrated by blending two special miscible PUs together, which do not have the hard/transition-segment structure individually but have two different melting temperatures. Below the melting temperature of the high melting temperature PU, one domain (the PU with a higher melting temperature) keeps elastic while the other (the PU with a lower melting temperature) is able to soften upon heating.

This category (Type II) may be called as dual-component mechanism (DCM). The working mechanism of DCM is as follows. Take a dual-domain polymer as an example. Refer to Fig. 2(II), in which the matrix is the elastic component and the inclusion is the transition component. Upon heating to above the transition temperature of the transition component, the inclusions soften. A force is applied to deform the material (illustrated by compression in Fig. 2II). While the matrix deforms elastically upon loading, the inclusions *flow* accordingly to accommodate the distortion. After cooling to below the transition temperature, the inclusions freeze and become hard. Upon removal of the constraint, the distorted inclusions, which are hard now, prevent the matrix from recovering its original shape. A residual strain is observed and elastic energy is stored in the matrix. This is the end of the programming process. Upon subsequent heating to above the transition temperature of the transition component, the inclusions soften again and thus the matrix is able to elastically bounce back and return to its original shape.

As we can see, many different versions can be developed from this mechanism. Practically, additional component may be included for the purpose of material modification.

Many extensions have actually been implemented in practice even without explicitly spelling out this concept.

One extension of the DCM is polymer blend, in which one polymer serves as the elastic component, while the other is selected to have the required transition temperature (within the required working temperature range). This type of SMP is listed as one distinct type in [35] under the name of polymer blend/filled polymer composite. According to Beloshenko et al. [35], Prof. BK Kim might be the pioneer in investigating the SME in polymer blends. In one of his reported works, PU was blended with polyvinyl chloride (PVC) [86]. A more recent example from the UK is acrylonitrile butadiene styrene/polycarbonate (ABS/PC) blend, which was developed for active disassembly of obsolete mobile phones at the required temperature for recycling [22].

As reported in [52], the SME has been examined in the mixtures of an elastomeric ionomer and low molar mass fatty acids and their salts [87], a non-woven fiber mat of a non-crosslinked polycaprolactone [88], and a matrix of poly (acrylic acid-co-methyl methacrylate) filled with cetyltrimethylammonium bromide [89].

These are extensions of the DCM, which might also be classified under the concept of shape memory hybrid (SMH) [66]. According to Huang et al. [66] and Sun et al. [23], SMH is essentially based on the same concept as DCM, but the components for selection are widened to include virtually any materials (including inorganic and metal/alloy, etc), so that tailored features and functions can be easily achieved. In addition, the interaction between the elastic component and transition component should be avoided or at least minimized by means of materials selection and processing selection. Consequently, the performance of the resulted hybrid can be well predicted in the early design stage. Fan et al. [90] demonstrated a few approaches to design and fabricate water-responsive SMHs.

The DCM is clearly revealed in a silicone hybrid with 30 % volume fraction of paraffin wax in Fig. 5. As expected, the micro-sized inclusions (paraffin wax) are deformed into elliptical shape according to the distortion during programming. Consequently, the temporary shape is able to be largely maintained after the elliptical shaped wax inclusions solidify. Upon heating again, the inclusions melt and recover the original circular shape, so that the silicone matrix eventually returns to the original shape.

It should be mentioned that a significant difference in the Young's modulus between the matrix and the inclusion may cause de-bonding at the matrix-inclusion interface. As revealed in Fig. 6a, upon stretching a silicone hybrid (loaded with 30 % volume fraction of an EVA based melting glue) to 50 % strain, we can clearly see many micro-sized eye-shaped features, in which the circular hard balls are melting glue (with a Young's modulus of 12 MPa). Each hard ball is actually within an elliptical shaped hole. After unloading, the elliptical shaped holes shrink but we still can see some gaps (Fig. 6b). Since the silicone is rubber-like and has a Young's modulus which is over 10 times lower (1 MPa) than that of melting glue, and the bonding stress between silicone and melting glue is only about 0.025 MPa, although the hybrid appears to be highly rubber-like with excellent

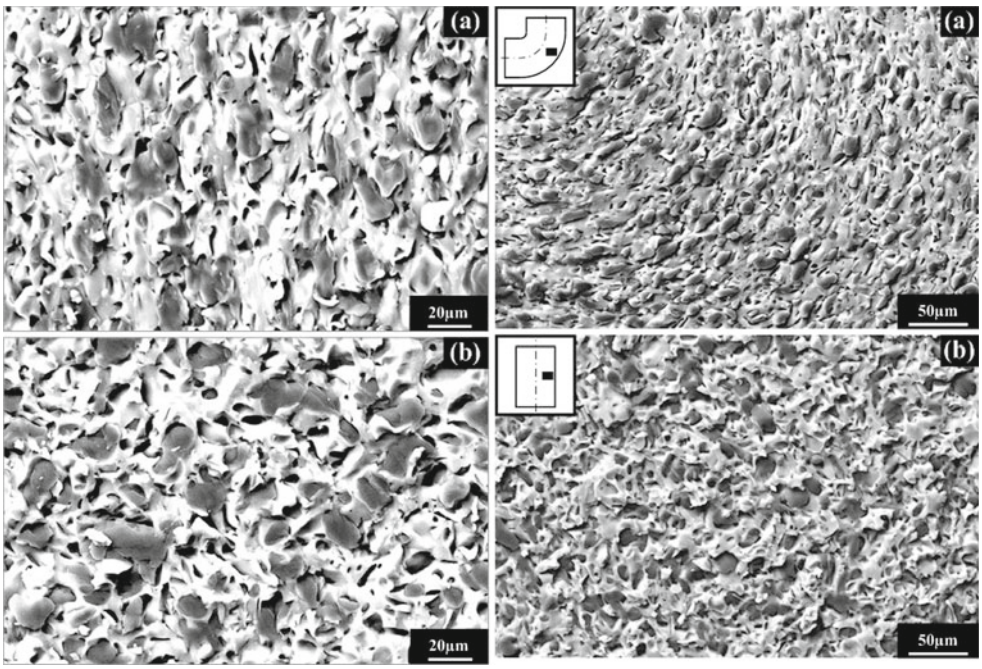

Fig. 5 The SME in silicone blended with 30 % volume fraction of paraffin wax (SEM images). Programmed by uniaxial tension (in the vertical direction) (I); and bending (the relative location of the examined area is marked) (II). **a** After programming; **b** after heating for shape recovery

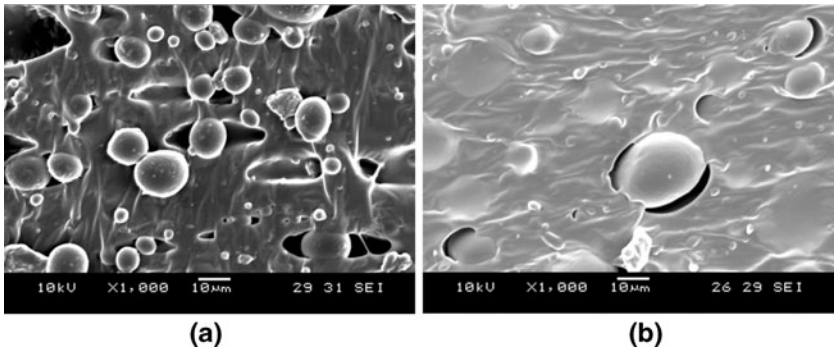

Fig. 6 SEM images of a silicone/melting glue hybrid. **a** Stretched at room temperature (along the horizontal direction); **b** after unloading

elasticity upon cyclic stretching [23, 66], there is some tiny residual strain after unloading due to these de-bonding induced gaps.

Partial-transition mechanism (PTM)

Above two types of mechanisms have already been explicitly or implicitly spelled out in the literature in different ways. All previous discussions about SMP classification are actually limited to within these two mechanisms only, although the exact chemical structures are often taken as the reference to determine which category a polymer should belong to. There is one type (III) which seemingly has never been mentioned, despite some of the reported experiments in the literature have actually implemented this mechanism, at least to a certain sense.

In [52], the influence of programming temperature on the recovery stress in constrained recovery (i.e., heating while the programmed shape is fixed) is discussed based on the experimental results. It is concluded that "Given its strong dependence on the applied thermomechanical conditions, recovery stress should not be considered as an intrinsic SMP properties" [52]. According to Sun et al. [91], if the influence of any time-dependent factors is ignored, the recovery stress from the elastic component is a constant. The additional contribution to the recovery stress is actually from the hard part of the transition component, which does not undergo the transition during programming. This hard part may be elastically deformed together with the elastic component during programming, so that this hard part functions as the elastic component as well.

This mechanism (Type III), named partial-transition mechanism (PTM) in Fig. 2, is also applicable to achieve the SME. As shown in Fig. 2(III), a polymer is partially heated so that a part of it (inclusions) softens. Upon deforming the polymer, the matrix (non-transition part, which is still elastic) is able to elastically deform, while the softened inclusions, just like the transition component in DCM, *flow* to accommodate the shape change. After cooling and removal of the applied constraint, the polymer is not able to return to its original height due to the constraint from the deformed inclusions (which are hard now). When being heated again to the previous heating temperature (precisely following the previous heating procedure), the inclusions soften again and thus, due to the elastic recovery of the matrix, the SME is observed.

Practically, this mechanism may work along or together with other two mechanisms. If working alone and the utilized phase transition is melting, the issue of thermal control becomes critical. Heating temperatures (both in programming and in thermally induced shape recovery) need to be carefully selected according to the precise transition progress-temperature relationship, and well-controlled to ensure high repeatability in terms of temperature distribution during thermal cycling. So called multiple-SME (will be discussed in details in Section "Further discussions") is a typical example, which essentially applies this mechanism.

The feasibility to realize the SME by implementing PTM is demonstrated in paraffin wax and melting glue (EVA based) by means of indentation test in Fig. 7. The utilized transition is melting in both materials. To avoid being confused by melting induced flowing which may virtually cause some-kind of shape recovery, an indentation-polishing-heating (IPH) approach is adopted to examine the SME in a convincing manner [10, 92, 93].

A 1 mm diameter steel ball is compressed slightly to make an indent atop a material that is heated to a predetermined temperature. This temperature is selected from within the melting temperature range of the material (refer to the differential scanning calorimeter (DSC) results which were conducted at a heating rate of 10 °C/min, and the exact heating temperatures were marked in the DSC figures, bottom row in Fig. 7). As we can see, for the paraffin wax, there are two peaks in its DSC curve upon heating. The selected temperature, 50 °C, is slightly over the starting point of the second peak; while for the melting glue, 55 °C is about the middle of the melting temperature range.

After cooling back to room temperature (about 22 °C) followed by removing the steel ball, the indents are scanned using a three-dimensional surface scanner (Taylor Hobson, top row in Fig. 7). The paraffin wax sample is slightly polished using a 1,200 grit sand paper till the indent just disappears, while a sharp pen knife is used to largely remove

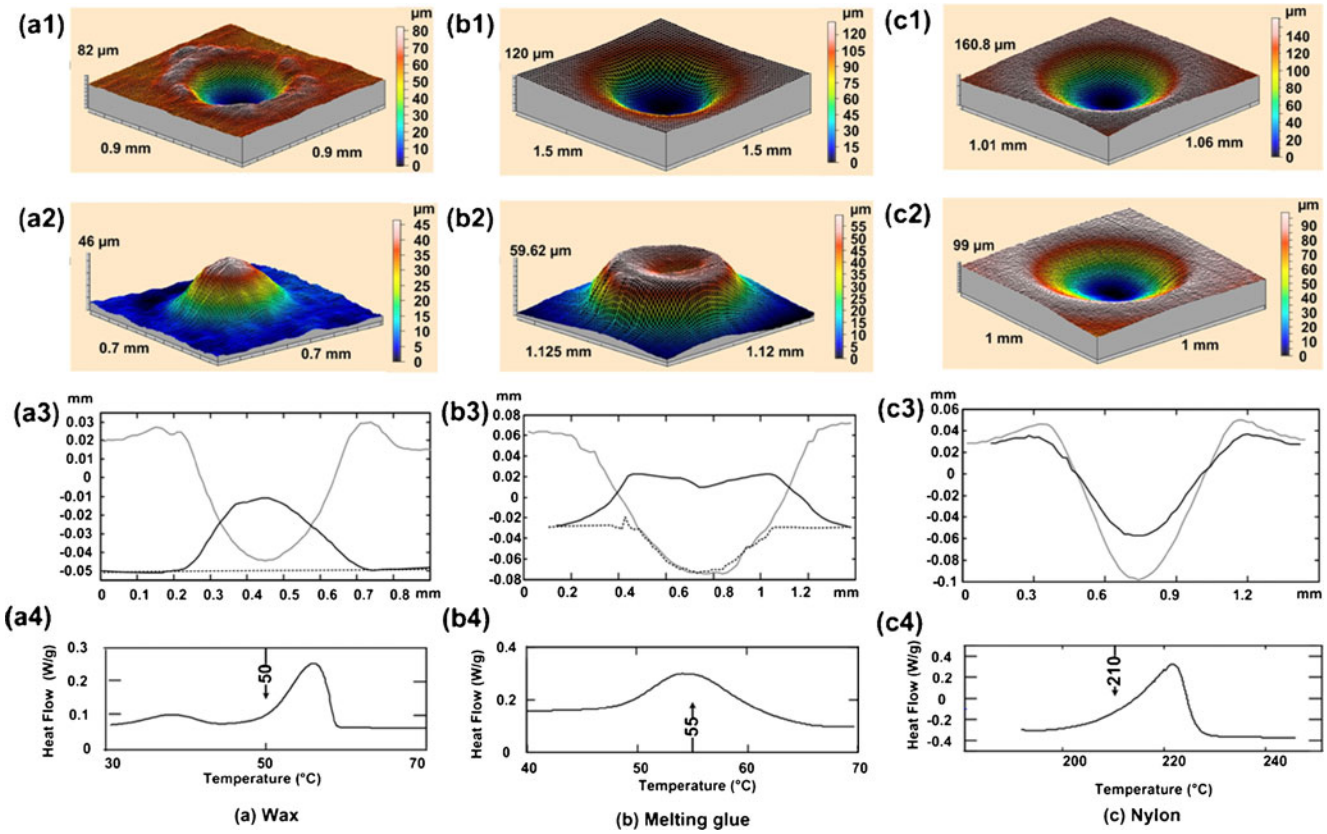

Fig. 7 Thermo-responsive SME demonstrated in (**a**) paraffin wax; **b** melting glue and (**c**) nylon. (1) After indentation; (2) after heating for shape recovery; (3) comparison of cross-sections; (4) DSC curve during heating

the indent atop the melting glue sample (refer to cross-sectional views in Fig. 7). After that, both samples are heated in an oven at their previous indentation temperatures for 5 min and being scanned again. We can see protrusions appeared atop both samples, which demonstrated the SME based on PTM.

It is obvious that the requirement for PTM is a dramatic change in stiffness in a reversible transformation. The exact shape memory performance depends on the applied strain and the temperature in programming.

Enabling the thermally induced SME in polymers

By utilizing the above three mechanisms either individually or in a combination manner, we can achieve the SME in almost any polymers, if not all.

When considering a new material, in many occasions, we may not have full knowledge about it, and/or the material itself might be very much complicated, e.g., it might be a mixture or a hybrid of many components (it is supposed to be microscopically uniform, at least, relative to the dimension scale in an application). On the other hand, from real engineering application point of view, the concern is more about achieving the SME to meet the required shape memory performance, without caring much about the exact working mechanism. As such, from engineering application point of view, an approach following PTM can be the starting point to enable the SME in any polymers.

A piece of nylon was used to demonstrate the implementation procedure in real practice. Refer to Fig. 7c.

- The first step is to conduct a DSC test to find out the location of the transition temperature range. Glass transition, melting and other phase transition are possible candidates for consideration. For this nylon, its melting temperature is in the range of 200 °C to 225 °C (Fig. 7c4).
- The next step is to select the heating temperature (within the transition range) for deformation (programming). To avoid (or at least to minimize) the damage to the elastic network, which reduces the shape recovery ability of the material, it is suggested to select a heating temperature which corresponds to the lower half of the transition range. Refer to Section "Fundamentals and optimization of the SME" for further discussion about this issue. Here, 210 °C is selected.
- Similar to the above mentioned two cases of paraffin wax and melting glue, a 1 mm diameter steel ball is used to make an indent atop nylon at 210 °C.

– After cooling back to room temperature, and removal of the steel ball, an indent is formed atop the piece of nylon.
– After heating to the previous heating temperature for indentation, the indent becomes shallower.

Obviously, shape recovery in the above experiment is partial only. The details on how to optimize the SME will be discussed in Section "Fundamentals and optimization of the SME".

In many applications, a full shape recovery is not particularly required. Take a retractable stent for example. One of the recent trends in the field of biomedical stents is so called degradable stent, which can be eventually fully absorbed by human body over time, which avoids the requirement for another operation to remove it. Some bio-degradable polymers, for instance, poly(vinyl alcohol) (PVA), polylactide (PLA), poly(ethylene glycol) (PEG) and poly(D,L-lactide) (PDLLA) etc, have been used for degradable stents in recent years [94, 95]. However, in some occasions, due to for instance, migration or severe infection, the degradable stents have to be taken out immediately. Although we have seen great efforts being devoted to developing bio-degradable SMP for stents [96–101], it is actually more ideal to enable the SME in existing biodegradable polymers, which have already been approved for medical applications and are readily commercially available, to avoid the tedious and long procedure of a new round of application for approval by medical authority. As shown in Fig. 8, a PLA spring (representing a spiral stent) is programmed into a larger diameter (Fig. 8b) and then twisted to fit into a catheter. After reaching the targeted location (via minimally invasive surgery), it is pushed out and automatically and elastically expands. In the event that an immediate removal is required, the PLA stent is heated slightly above the body temperature so that it shrinks (Fig. 8c). Subsequently, it can be pulled back into the catheter and removed from human body again by means of minimally invasive surgery. Although the shape recovery is not 100 %, those stents are still acceptable as long as they can be fitted comfortably into a catheter again.

It should be pointed out that depending on the exact polymer and its thermo-mechanical properties, the actual programming procedure might be modified accordingly, just like that in SMAs, which can be programmed either in high temperature austenite phase or low temperature martensite phase [26, 27]. For examples, ductile PU and PC may be programmed in the glassy state (e.g., [29, 91]), while for brittle polystyrene (PS) and PMMA, programming in the glassy state is more likely only possible if the applied loading is in compression (e.g., [13, 29]). However, for ductile polymers, necking like non-uniform deformation may occur in uniaxial tension, while for brittle polymers, even stretching at temperatures slightly lower than the transition finish temperature may cause micro-scale fracture [91, 102]. In Rodriguez et al. [103], programming at low temperatures and then heating for shape recovery is named as the "reversible plasticity SME" in order to distinguish it from programming at high temperatures.

We may take note that the PTM is applicable to enable the thermally induced SME in other types of materials as well, such as metals and alloys, which are not within the traditional SMM family. The requirement for PTM is a dramatic change in stiffness in a reversible transformation. The exact shape memory performance depends on the applied strain and the temperature in programming, and can be tuned for optimized performance.

Chemically induced SME

A few SMPs which respond to water/moisture have been developed (e.g., [37, 104–108]). Recently, Kumpfer and Rowan [63] have synthesized a covalently cross-linked metallo-supramolecular polymer which can be activated upon immersing into methanol.

The programming procedure for the chemo-responsive SME is essentially the same as that in the thermo-responsive SME as discussed above. However, instead of heating to above the transition temperature to activate the SME, the approach applied to trigger the chemo-responsive SME is to soften/dissolve the transition component (Type II in Fig. 2) or, as opposed to heating to activate the transition, the transition temperature in pre-programmed polymers is lowered instead (Types I and III in Fig. 2).

Softening

As shown in Fig. 9, two pieces of PU SMP wires (indicated as original) are immersed into 22 °C water and ethanol, respectively. The wire immersed in the water has a nominal T_g of 35 °C, while the other immersed in the ethanol has a nominal T_g of 55 °C. Both polymers (MM3520 and MM5520) were bought from SMP Technologies, Inc.,

Fig. 8 Thermo-responsive SME in a commercial PLA

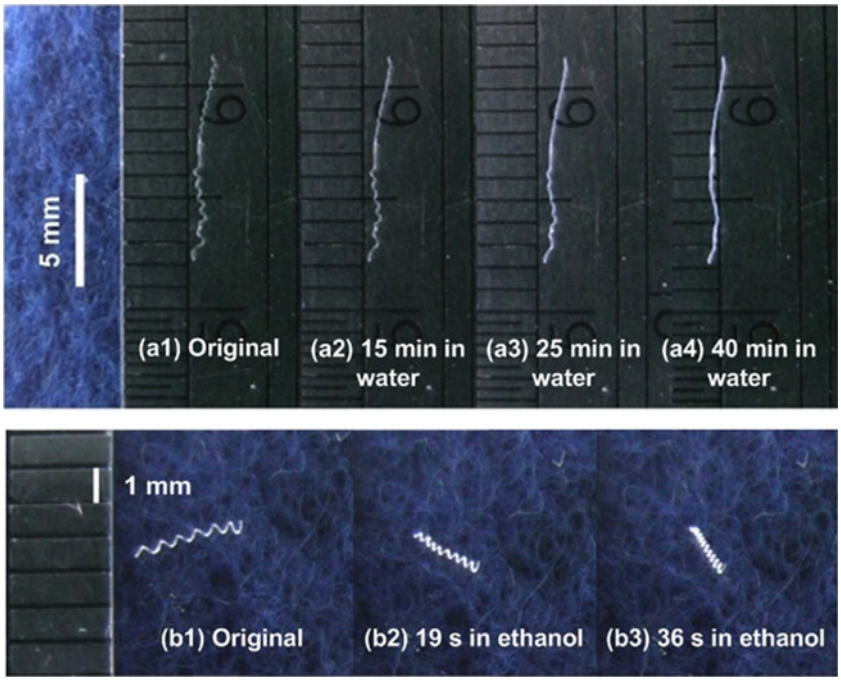

Fig. 9 Chemo-responsive SME in PU SMP. Top: in 22 °C water (T_g: 35 °C); bottom: in 22 °C ethanol (T_g: 55 °C)

Japan. The one immersed in the water (Fig. 9a), although it has a 20 °C lower T_g than the other, takes about 40 min to straighten; while the other immersed in ethanol (Fig. 9b) reacts much faster (shape recovery finished within about 30 s only).

According to Yang et al. [109] and Huang et al. [110], upon immersing into room temperature water (about 22 °C), the T_g of both MM3520 and MM5520 can be gradually reduced by up to 30 °C due to the plasticizing effect of the absorbed bound water on hydrogen bonding evidenced by the shift of C=O stretching and N-H stretching measured by Fourier transform infrared (FTIR) spectroscopy as revealed in Fig. 10 (for MM3520). Figure 10 also reveals similar shift in C=O stretching and N-H stretching in PU SMP (MM5520)

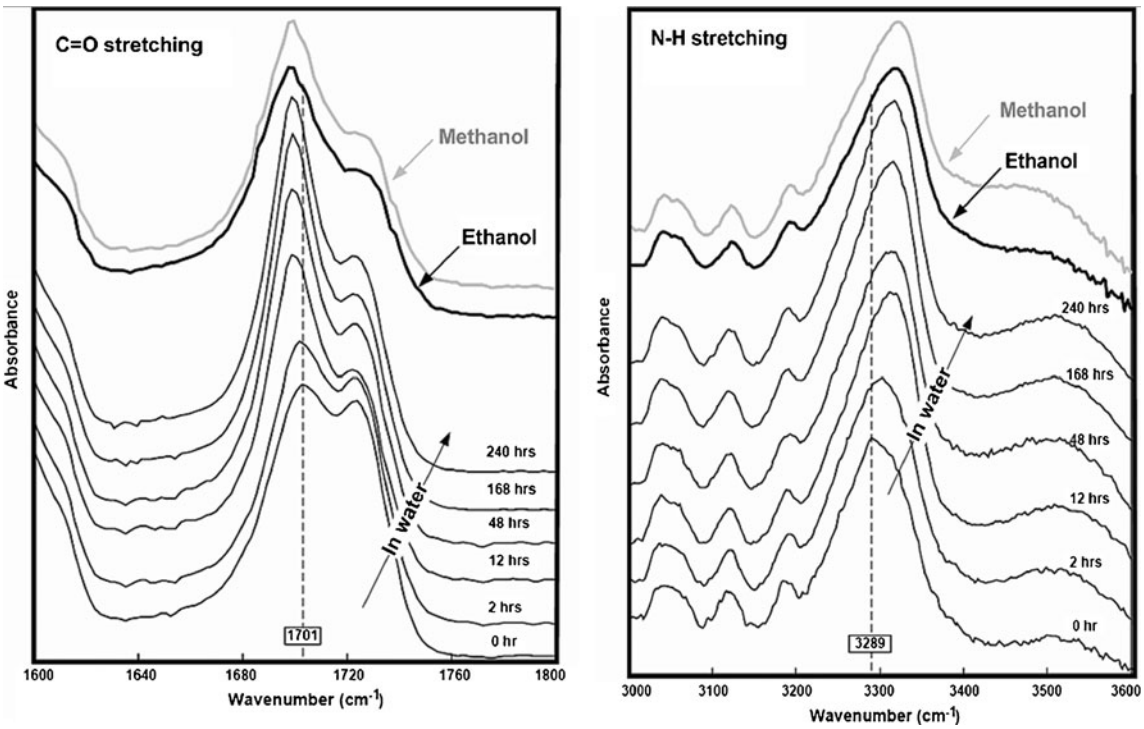

Fig. 10 Shift in C=O stretching (*left*) and N-H stretching (*right*) upon immersing into room temperature water (MM3520) and ethanol/methanol (MM5520)

after being immersed in ethanol and methanol. It is worth taking note that upon immersion into methanol, this type of PU SMP, which is thermo-plastic, quickly dissolves in it.

The influence of water absorption on T_g can be quantitatively determined [111]. A typical example of MM3520 is revealed in Fig. 11. It is obvious that with a longer immersion time in water, T_g reduces further (further evidenced by the shift in C=O stretching and N-H stretching in Fig. 10). Upon gradually heating, the SMP becomes lighter but there is not much change in T_g at all, until it is heated above a certain temperature. From then on, with further increase in temperature, the weight of SMP drops while T_g increases continuously. It is found that the absorbed water actually includes two parts, namely free water and bound water (Fig. 12). While free water does not affect T_g, and can be removed upon heating to below 120 °C, bound water has strong influence on T_g and can only be removed upon heating to over 120 °C. The latter indicates that by heating to remove the absorbed water, the SMP can return to its original state/condition (evidenced by the experimental results reported in [109]).

The influence of water on T_g can be utilized for water activated SME, for programmed shape recovery by means of introducing a gradient T_g in a piece of SMP (further discussed in Section "Multiple-SME"), or for reduction of T_g before applying a lower heating temperature for activation (chemically tuning T_g, without altering the chemical composition in synthesis).

In order to have enough stiffness in working conditions, the transition temperature of a SMP should be higher than the environmental temperature. A piece of PU SMP (MM5520) is straightened first (Fig. 13a–b). Since its nominal T_g is 55 °C, it is strong enough to be inserted into a cluster of toad eggs at room temperature (around 20 °C to 22 °C) without much difficulty even without using any special tools (Fig. 13c). After 7 days, its T_g is expected to drop by as much as 30 °C (maximum), which is still above the ambient temperature, so that we only see some slight shape recovery as shown in Fig. 13d. By heating to 37.5 °C, which is still within the safe temperature range without worrying over the risk of killing the toad eggs, we can see great shape recovery in the PU wire. This experiment demonstrates that by selecting a right chemical, one may tailor the transition temperature of a polymer. This approach could be an alternative to the chemical composition tuning, which is a more popular practice at present, to modify transition temperatures.

Various types of polystyrene (PS) have been used based on their thermo-responsive SME, from traditional packaging to surface patterning and micro-machining of microchannels [9, 11, 13, 92, 93, 112, 113]. Lv et al. [114] has used dimethylformamide (DMF) to trigger the SME in PS SMP. In Fig. 14, a piece of thermo-set PS (4.5 mm thick, from Cornerstone Research Group, USA) was programmed by bending at 60 °C into the temporary shape. After being kept in room temperature acetone for 16 h, it became straight again but actually longer in length. This observation reveals a certain level of swelling in chemically induced SME in this polymer.

If *swelling* is significant, eventually a thermo-plastic polymer may be fully dissolved, while a thermo-set polymer becomes a gel with a huge volume expansion. Since we can almost always find a chemical to soften a polymer without causing much volume change, we may claim that all polymers are also naturally chemo-responsive.

For dual-component materials, we may select a chemical which softens the transition component only. On the other

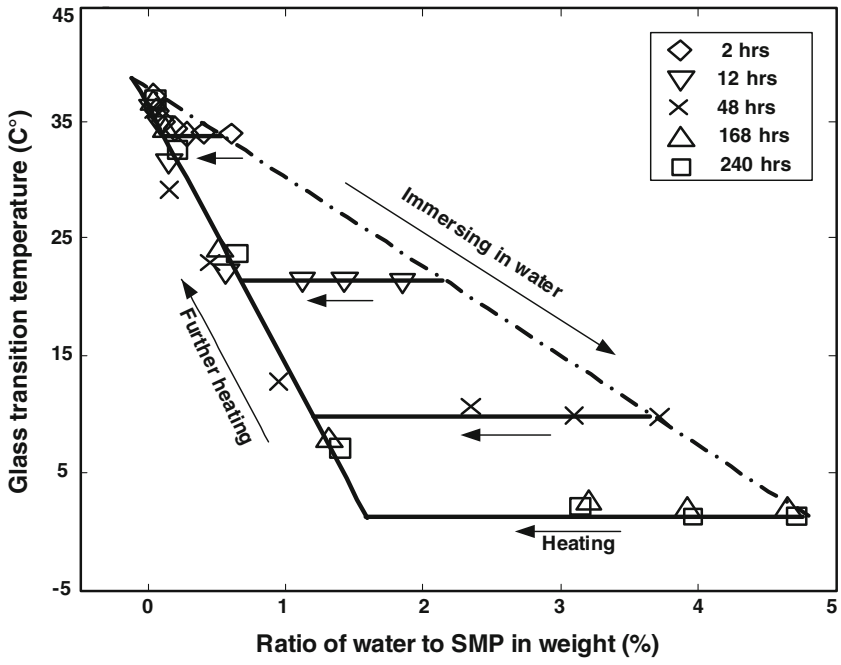

Fig. 11 T_g vs. ratio of water to SMP in weight %. Reproduced with permission from American Institute of Physics [111]

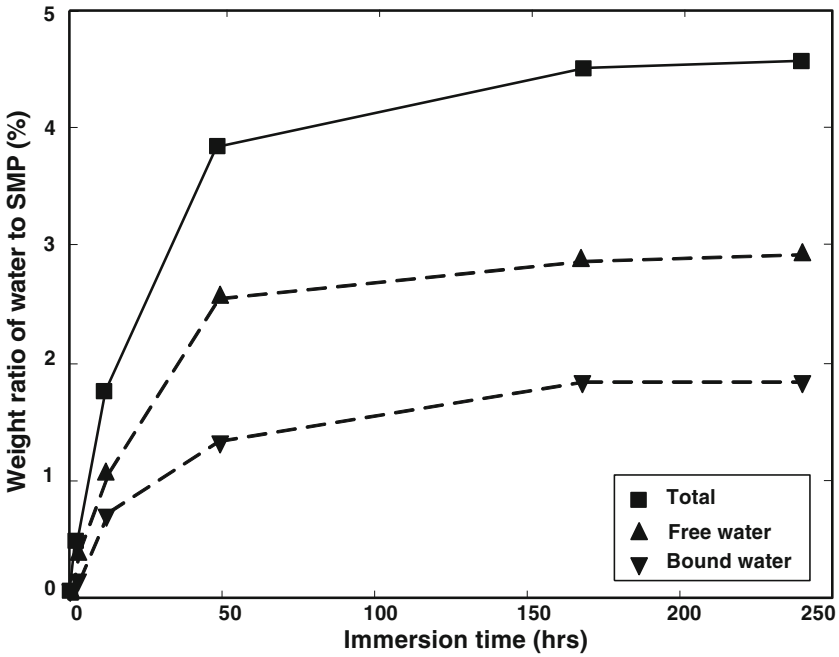

Fig. 12 Ratio of water to SMP in weight percentage vs. immersion time. Reproduced with permission from Elsevier Ltd. [109]

hand, we can design a special dual-component material which has a transition component that can be softened by a particular chemical under its working environment. This is to design a material with integrated both sensing and reaction functions.

Mechanical instability induced buckling

The thermo-responsive SME in poly(methyl methacrylate) (PMMA) has been reported in the past, but only limited to small strain range [47, 48]. In addition to thermally induced shape recovery, Harmon et al. [115] have reported methanol induced shape recovery in PMMA, but again only within small strain range. A recent study reveals a recoverable strain in the order of 100 % in PMMA [34]. Unlike many other polymers (such as the above mentioned PUs), after immersing PMMA into ethanol, we can clearly see a line which indicates the penetration/diffusion depth of ethanol (Fig. 15). This line moves inward further with a prolonged immersion time [34]. Hence, we can see two different T_gs, one for the part with ethanol and the other for the part

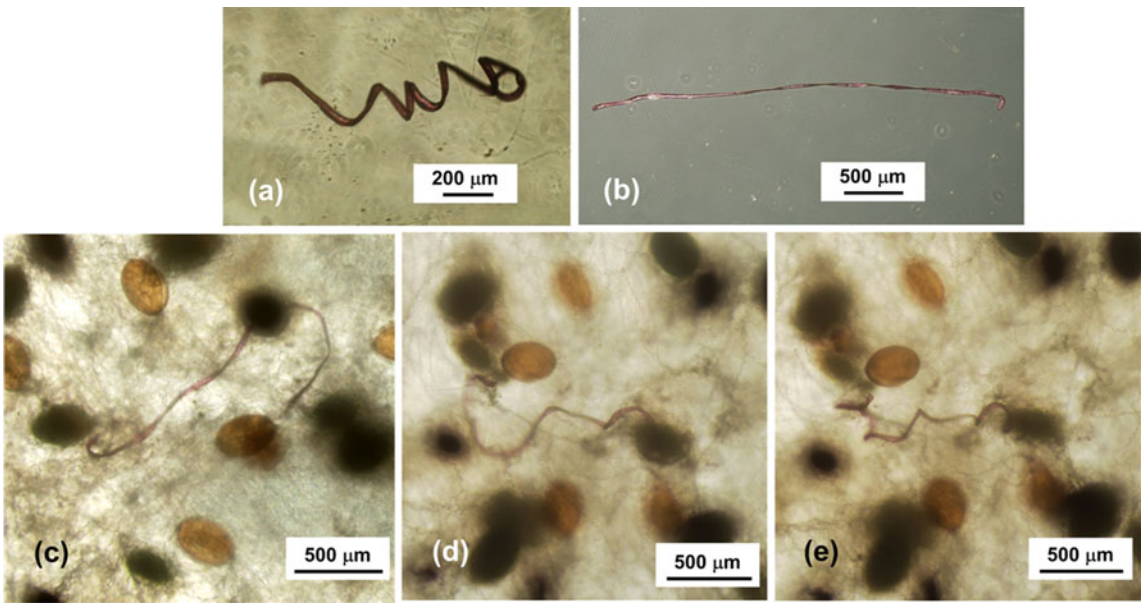

Fig. 13 **a** Original shape; **b** after straightening; **c** after inserting into a cluster of toad eggs; **d** after seven days in room temperature water; **e** after heating to 37.5 °C

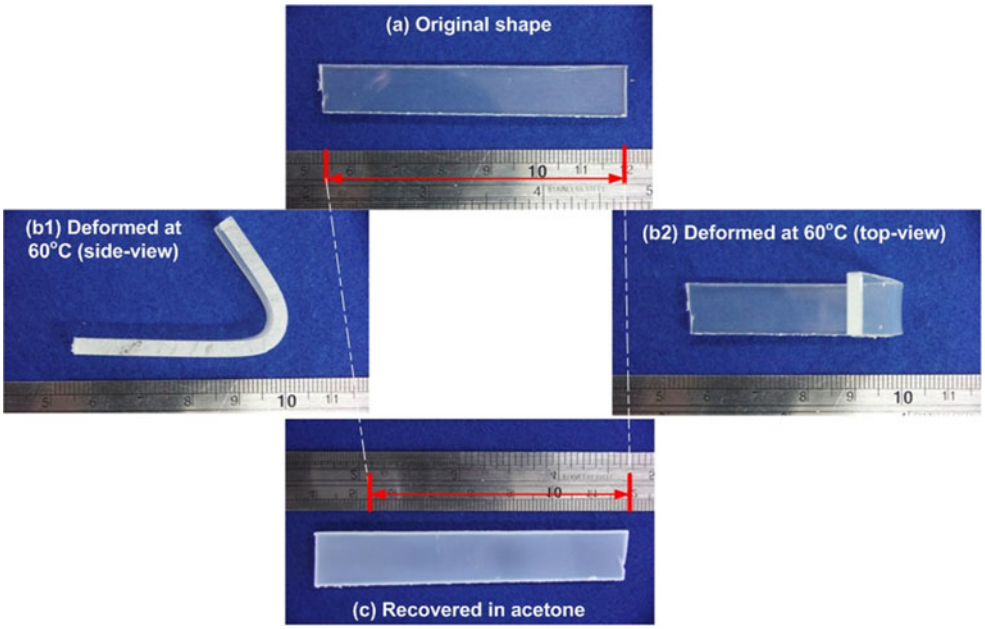

Fig. 14 Shape recovery in a piece of pre-bent PS upon immersing into acetone for 16 h

without ethanol, instead of a gradually decreasing T_g as in PUs after being immersed in the water for a different periods of time.

Within the large deformation regime, mechanical instability may turn to be an important issue. As shown in Fig. 16 (I), a piece of PMMA (right part) is stretched at above its T_g, so that after programming, the length of the right part of the PMMA is more than doubled. Upon gradually heating, instead of gradually shrinking back to the original dimensions, at about 110 °C, which is around its T_g, the sample becomes curved. Upon further heating, the sample gradually recovers its original shape. One may suspect that the cause of curving at 110 °C is due to temperature gradient, which is common in real practice, and thus the shape recovery is not uniform. Since one side (surface) of the sample recovers more than the other side (surface), the sample becomes curved. In another experiment, at above the T_g the sample is stretched slightly and then bent during programming before being immersed into room temperature ethanol (Fig. 16II). As expected, the PMMA straightens and shortens gradually and recovers its original shape after 120 h. In the last experiment, the sample is severely stretched at above its T_g before being placed inside room temperature ethanol (Fig. 16III). The sample curves first and then shrinks, but fails to return to its original shape and dimension, even after being heated inside 100 °C boiling water for 10 s. About full shape recovery is observed after being heated to 150 °C, which is well above its glass transition temperature range.

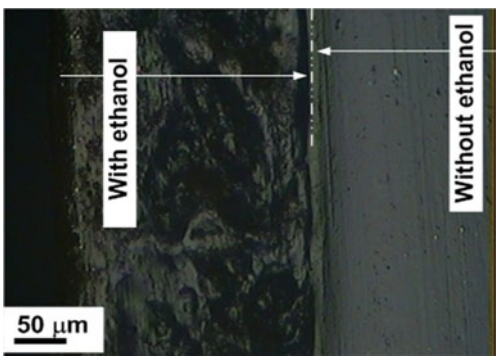

Fig. 15 Penetration line of ethanol in PMMA

In [34], the fundamental reason for curving of PMMA upon heating and immersing into ethanol is explained as the mechanical instability induced buckling. Derived from the Euler buckling condition for columns, and after ignoring the influence of swelling, the buckling condition for pre-stretched PMMA upon immersing into ethanol is obtained. It is concluded that with a higher pre-strain, buckling occurs earlier. This is confirmed by the experimental results reported in [34]. It is also revealed that when other conditions are the same, buckling starts earlier in a longer sample.

We also notice significant swelling in a long pre-stretched PMMA, which prevents full shape recovery of PMMA by means of immersing into ethanol only. This is due to the pre-strain/stress-enhanced swelling [115, 116]. It is found that heating to release the absorbed ethanol (this is particularly effective at high temperatures, e.g. at above T_g, in terms of a shortened heating time) is a practical approach to achieve full shape recovery. Additionally, when we compare the experimental results of Fig. 16(II) and (III), it is clear that swelling ratio is affected by the magnitude of pre-strain.

Mechanical instability in the thermally induced SME may be minimized (if not avoided) by maintaining high uniformity in temperature distribution. However, in the case of chemically induced SME, given the non-uniformity

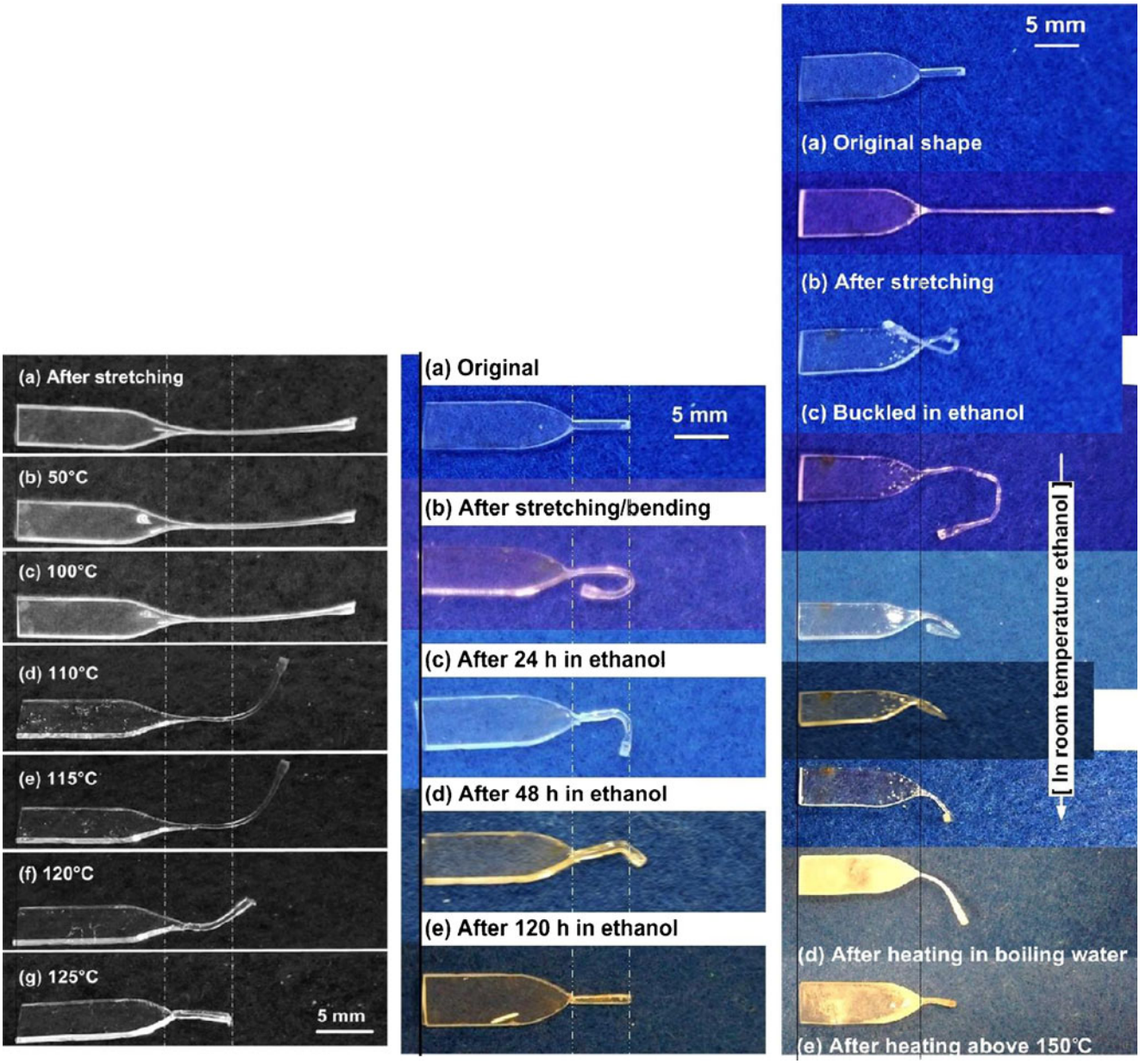

Fig. 16 Shape recovery in PMMA by heating (I), immersing into ethanol (II), and immersing into ethanol followed by heating (III)

nature of chemical penetration/diffusion, it might be difficult to eliminate mechanical instability. The fundamental solution is to design the configuration of a polymer element to avoid the conditions which may cause mechanical instability.

Dissolving

Instead of softening, in dual-component materials, shape recovery may be induced by removing the transition component, so that the elastic component can freely release the elastic energy stored during programming.

Figure 17 is SEM image showing the dispersion of sodium acetate trihydrate (50 vol.%) within a silicone matrix. Apart from large aggregations, we can see small sodium acetate trihydrate particles which essentially serve as micro channels to bridge these aggregations. It is well known that sodium acetate trihydrate is highly dissolvable in water and has a melting temperature at about 60 °C. On the other hand, silicone is chemically and physically stable from −20 °C to 120 °C.

As shown in Fig. 18, a hybrid ring with circular shape, which is made of silicone and sodium acetate trihydrate, is programmed at above 60 °C into a star shape. After being

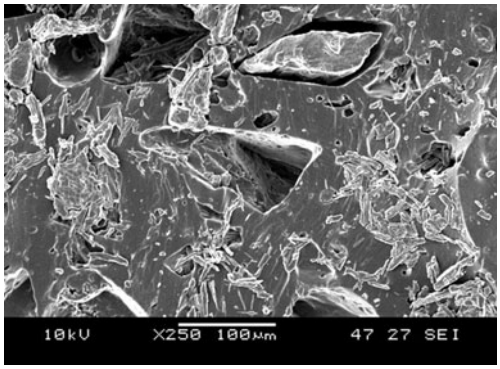

Fig. 17 Typical SEM image showing the dispersion of sodium acetate trihydrate (at 50 vol.%) within silicone. Reproduced with permission from Budapest University of Technology and Economics [90]

immersed into room temperature water, the ring gradually recovers its original circular shape. The actual recovery speed can be controlled by varying the volume fraction of sodium acetate trihydrate.

Sodium acetate trihydrate, which is stiffer (as compared with silicone) but much more brittle, belongs to inorganic crystal. Highly water dissolvable polymers, such as PEG, can be used to replace sodium acetate trihydrate, so that the resulted material is biocompatible and still being responsive to water. Acetone is able to quickly dissolve PU, so that acetone may be used as the stimulus for a dual-component material, in which PU is the transition component, while the elastic component should be inactive to acetone. There are many combinations, which are possible to meet the requirements on the exact chemical stimulus, strength, recovery speed and recoverable strain etc.

Recovery speed

In the thermo-responsive SME in polymers, the recovery speed is mainly dominated by the speed of heating, although thermal conductivity, latent heat (if applicable), specific heat, heat transfer (conduction, convection and maybe radiation) etc should play certain roles, depending on the exact setup.

According to Petrovic et al. [117], the interaction parameter, χ, between solvent (chemical) and polymer may be determined by

$$\chi = (\delta_2 - \delta_1)^2 V_1 / RT \quad (1)$$

where δ_1 and δ_2 are solubility parameters of solvent and polymer, V_1 is the molar volume of solvent, R is gas constant, and T is absolute temperature. As we can see, given a fixed temperature, χ increases with the increase in difference of solubility parameter between solvent and polymer, and the increase of molar volume of solvent.

Depending on the exact situation, there are at the most three diffusion speeds which are influential in governing the shape recovery speed in chemo-responsive SME, namely the diffusion speed of solvent in elastic component, the diffusion speed of solvent in transition component, and the diffusion speed of transition component in solvent surrounding the polymer sample (only for dissolving case). In the case of dual-state material, there is only one speed, i.e., the diffusion speed of solvent in polymer.

It is possible to design a dual-component material, in which a solvent has swept throughout the entire elastic component while the interaction with the transition component is still well lagged behind. As shown in Fig. 15, in some materials, there might be a clearly visible penetration line.

The topic of the recovery speed in chemo-responsive SME in polymers is essentially similar to that in controlled drug release, which has attracted great attention in recent years (e.g., [118–123]).

Unconventional stimuli

So far the development in chemo-responsive polymers is seemingly limited to utilizing chemicals for softening

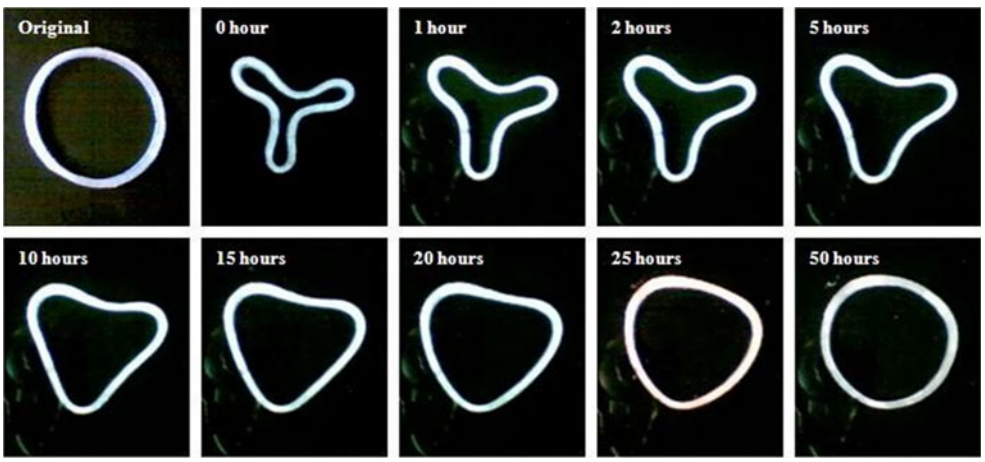

Fig. 18 Shape recovery in a silicone hybrid ring filled with 50 vol.% of sodium acetate trihydrate upon immersing into room temperature water. Reproduced with permission from Budapest University of Technology and Economics [90]

actually by physical meaning, e.g., plasticizing (with negligible volume expansion), swelling (with limited volume expansion. Gel will be discussed in Section "SME in gel, protein and DNA") and dissolving (with infinite volume expansion). In addition to degradation which is applicable to all degradable materials including polymers, it should be possible to soften the transition component by other means, such as chemical decomposition and bio-reaction.

An interesting area to explore within the topic of chemo-responsive SME is to utilize those polymers developed from microorganisms and plants etc., known as bio-plastics, rather than fossil-fuel plastics which are derived from petroleum (e.g., [124–126]). Bio-plastics are naturally biocompatible and most likely easy in biodegradation. Decomposition by bacteria can be an alternative to soften/remove the transition component [127]. Furthermore, enzyme may be used to decompose protein based bio-plastics [128] (the SME in proteins will be discussed in Section "SME in gel, protein and DNA").

Fundamentals and optimization of the SME

Instead of discussing chemical composition tuning which is very much dependent on the individual type of polymer, we investigate the generic principles in the optimization of the SME from the aspects of mechanics and mechanism design. Here, thermo-responsive SME is taken as an example in the discussion. Chemo-responsive SME may be discussed in a similar way [129].

From the mechanical function point of view, *cross-linked* net-points and switch segments in DSM, which were pointed out by Xie T [52] as the two structural requirements for the SME, are roughly corresponding to the elastic component and transition component in DCM and PTM, respectively. Consequently, the SME in polymers under all three working mechanisms can be integrated and discussed under one single umbrella, i.e., a material system, which consists of an elastic component (may be simplified as matrix in the discussion) and a transition component (may be considered as inclusions).

It is obvious that the elastic component with good elasticity (to avoid permanent distortion, which is supposed to be irrecoverable), and the transition component which relatively easily being "plastically" distorted (and the residual deformation can be largely maintained) are two apparent conditions. By closely examining the behavior of this matrix/inclusion system, we should be able to work out some generic conclusions, which may serve as the principles to follow in the design/synthesis and optimization of individual materials.

Fundamentals and optimization of the key parameters which are influential on the shape memory performance are discussed individually in this section.

Again, for simplicity, time-dependent parameters and phenomena are ignored and we also omit the influence of thermal expansion. The following discussion is essentially based on engineering strain and engineering stress.

Shape fixity ratio

Shape fixity ratio is a measure of the ability of a SMM to keep the shape change after programming. There are two commonly applied testing approaches to determine the shape fixity ratio of a SMM. One is bending test by measuring the remaining bending angle against the applied maximum bending angle in programming, the other is uniaxial tension or compression test by calculating the ratio between the remaining strain after programming and the maximum strain applied in programming [74, 130–134].

We consider a representative unit of a dual-component polymer as shown in Fig. 19a, in which the elastic component (represented by a spring) is in parallel to the transition component. By examining the response of this unit, the performance of the whole piece of the material can be revealed.

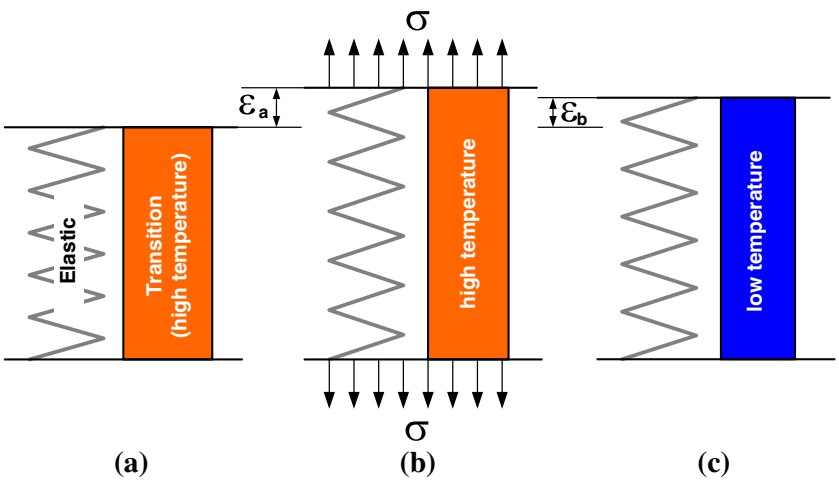

Fig. 19 Representative unit of a dual-component polymer. **a** Free-standing at above the transition temperature; **b** stretching at above the transition temperature; **c** after cooling and removing the applied constraint

As the first step, we discuss the case of programming at above the transition temperature (i.e., the basic programming procedure as illustrated in Fig. 2II) but by means of unaxial tension.

To further simplify the situation, we assume the transition occurs within a very narrow temperature range, so that we only need to consider two temperatures, one is above the transition temperature (high temperature), and the other is below the transition temperature (low temperature). The mechanical behaviors of the elastic component and transition component at high and low temperatures are illustrated in Fig. 20. Note that since uniaxial tension is applied in the programming, the elastic component is always in tension. We assume it is always linear elastic (Young's modulus: E^e; cross-sectional area: A^e). For the transition component, above the transition temperature, it is easy to flow. We assume it is perfect plasticity with a yield stress of σ_a^t. However, after programming, it is in compression below the transition temperature to maintain the remaining strain against the stretched elastic component. The Young's modulus of the transition component is E^t, the cross-sectional area is A^t, and the yield stress in compression is σ_y^t.

Refer to Fig. 19. After being stretched to a maximum strain of ε_a (marked as a in Fig. 20 along $\varepsilon-$axis) at above the transition temperature, the material is cooled to below the transition temperature. After the constraint is removed, the residual strain, ε_b (marked as b in Fig. 20 along $\varepsilon-$axis), may be expressed as,

$$\varepsilon_b = \frac{A^t\left(E^t\varepsilon_a - \sigma_a^t\right)}{A^eE^e + A^tE^t} \tag{2}$$

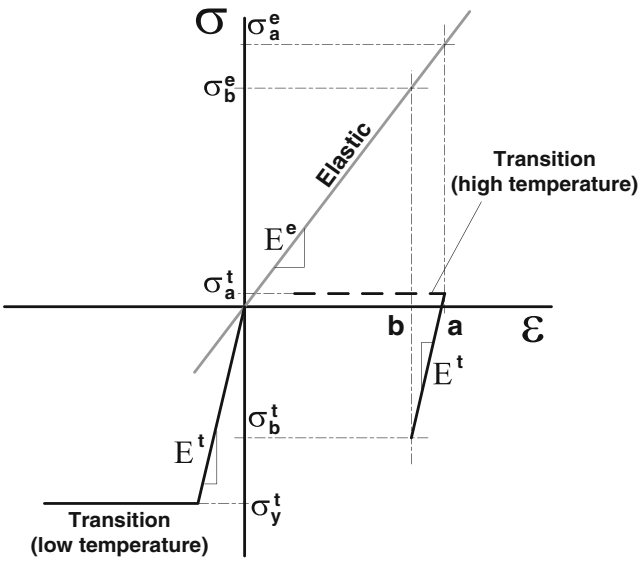

Fig. 20 Illustration of stress vs. strain relationships of the elastic component and transition components at above and below the transition temperature

To maximize ε_b in Eq. (2) for better shape retaining means that $\varepsilon_b \to \varepsilon_a$, which requires that,

$$\cdot\ \sigma_a^t \text{ is min imized and } A^eE^e \ll A^tE^t \qquad \text{(Condition I)}$$

We ignore the possible Bauschinger effect due to reversion in loading direction in the transition component in this study. Therefore, to avoid yielding of the transition component in compression, which reduces shape fixity ratio, we need to have,

$$\cdot\ \sigma_y^t < -\frac{E^t\varepsilon_a - \sigma_a^t}{1 + \frac{A^tE^t}{A^eE^e}} \qquad \text{(Condition II)}$$

Although Conditions I and II are derived based on some simplifications and assumptions, they provide guidelines in materials selection for the elastic and transition components and the requirement on geometrical dimensions (volume ratio. Refer to Section "Volume fraction of transition component" for further discussion).

The above discussion is based on the assumption that programming is conducted at high temperatures (transition component is fully softened). Programming at lower temperatures should require a higher stress to reach the same maximum strain, while the resultant residual strain is less due to higher elastic recovery [91].

Figure 21a reveals the maximum compressive stress in programming vs. the programming temperature curves of a commercial biodegradable polymer (BIOCOM® DPEF9910 multi-degradable resin, from NAFT Asia Biodegradable Plastics Corp., Singapore). Two maximum strains were applied, namely 5 % and 10 %. The selected temperatures for programming are around the melting transition. It is confirmed that with an increase in programming temperature, the maximum compressive stress decreases monotonically at both maximum strains. In Fig. 21b, the shape fixity ratio vs. programming temperature relationships are shown. A quasi-linear relationship is observed between the shape fixity ratio and programming temperature at both 5 % and 10 % strains. It reveals that a higher maximum programming strain results in a higher shape fixity ratio. The shape recovery behavior of this polymer will be discussed in Section "Shape recovery ratio and multiple-transition".

In another set of experiments, polyether ether ketone (PEEK) thin films with a thickness of 0.1 mm were uniaxially stretched to different maximum strains at room temperature at a strain rate of 0.1 %/s. DSC result (Fig. 22a) reveals that there are two transitions in this thermo-plastic PEEK, one is glass transition at around 145 °C, and the other is melting transition at above 300 °C. It is noticed that this thin film PEEK becomes warped when heated to above 300 °C. The shape fixity ratio vs. the maximum pre-strain relationships are shown in Fig. 22b. Apparently, a higher programming strain results in a higher shape fixity ratio.

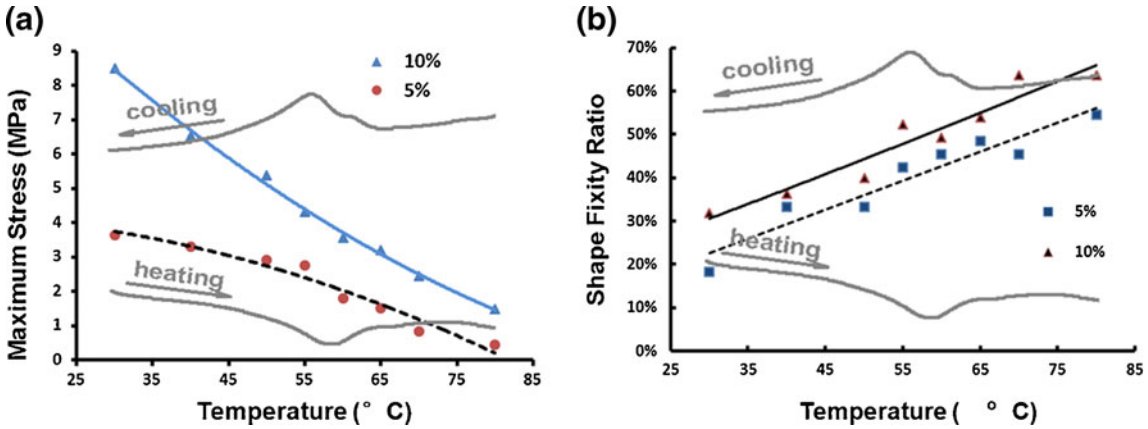

Fig. 21 Programming a commercial biodegradable polymer at different temperatures by uniaxial compression to maximum strains of 5 % and 10 %. **a** Maximum compressive stress vs. programming temperature relationships; **b** shape fixity ratio vs. programming temperature relationships. Embedded grey curves are DSC results at a heating/cooling rate of 10 °C/min

Thermally induced SME (Fig. 22c) will be discussed in Section "Shape recovery progress".

In fact, both the biodegradable polymer and PEEK film mentioned above are not able to fully recover their original shape upon heating. Hence, it is necessary to know the strain limit in programming.

Maximum strain in programming

SMPs with a very high recoverable strain have been developed (e.g., [135, 136]). By means of exquisite control over crosslinking density in a SMP, it is found that increased crosslink density leads to a decrease in the maximum strain to failure [137]. In this section, we discuss the strain limit in programming at above the transition temperature, since this is the case that the strain in programming and hence, the SME can be maximized. Another reason is due to the complex interaction between the elastic and transition components upon distortion at low temperatures, which causes the difficulties to derive a simple model for all kinds of situations.

What recently reported by Feldkamp and Rousseau [138] in an epoxy SMP shows that a higher fracture strain can be achieved by deforming at a lower programming temperature. However, in general, depending on the nature of a polymer, programming at lower temperatures may have a higher chance to deteriorate the SME by means of micro fracture or brittle fracture, or lower shape fixity ratio and reduced shape recovery (e.g., [91, 102]).

Consider an ideal situation as illustrated in Fig. 23, in which an elastic foam/network is fully filled with a transition component. We use this simplified two dimensional model to investigate strain limit based on pure geometrical analysis.

Assume that at high temperatures (above the transition temperature) the transition component is able to flow easily but non-compressible. Consider a unit cell, which is subjected to a point load which is applied in the vertical direction (Y) as shown in Fig. 23. Upon compressing, the condition that the transition component can easily flow but is non-compressible requires,

$$\left(1-\varepsilon_y\right)\times\left(1+\varepsilon_x\right)=1 \tag{3}$$

where ε_x and ε_y are the resulted strains in the horizontal (X) and vertical (Y) directions, respectively. The elastic component should elastically deform (uniaxial extension) accordingly to ensure that there is not any volume change in the transition component, i.e.,

$$\left(1-\varepsilon_y\right)^2+\left(1+\varepsilon_x\right)^2=\sqrt{2}\left(1+\varepsilon_L\right)^2 \tag{4}$$

where ε_L is the elastic strain in the elastic component. Subsequently, we have ε_L and ε_x in terms of ε_y as,

$$\varepsilon_L=\frac{\sqrt{2}}{2}\left[\left(1-\varepsilon_y\right)^2+\frac{1}{\left(1-\varepsilon_y\right)^2}\right]^{1/2} \tag{5}$$

and

$$\varepsilon_x=\frac{1}{1-\varepsilon_y}-1 \tag{6}$$

Figure 24 plots the variation of ε_L and ε_x in terms of ε_y. Since the elastic component should be loaded within its elastic range to ensure full shape recovery, based on the maximum elastic strain of the elastic component, we can predict the strain limit in programming. Figure 24 is plotted for the situation of unaxial compression. By re-plotting it as ε_L against ε_x, we can determine the case of uniaxial tension. Other loading situations (and even in three-dimensional cases) can be estimated in a similar way.

Of course, the above discussion is for the estimation to catch the fundamentals, since the real situation is much more complicated. However, we can easily conclude that a higher programming strain (and consequently higher

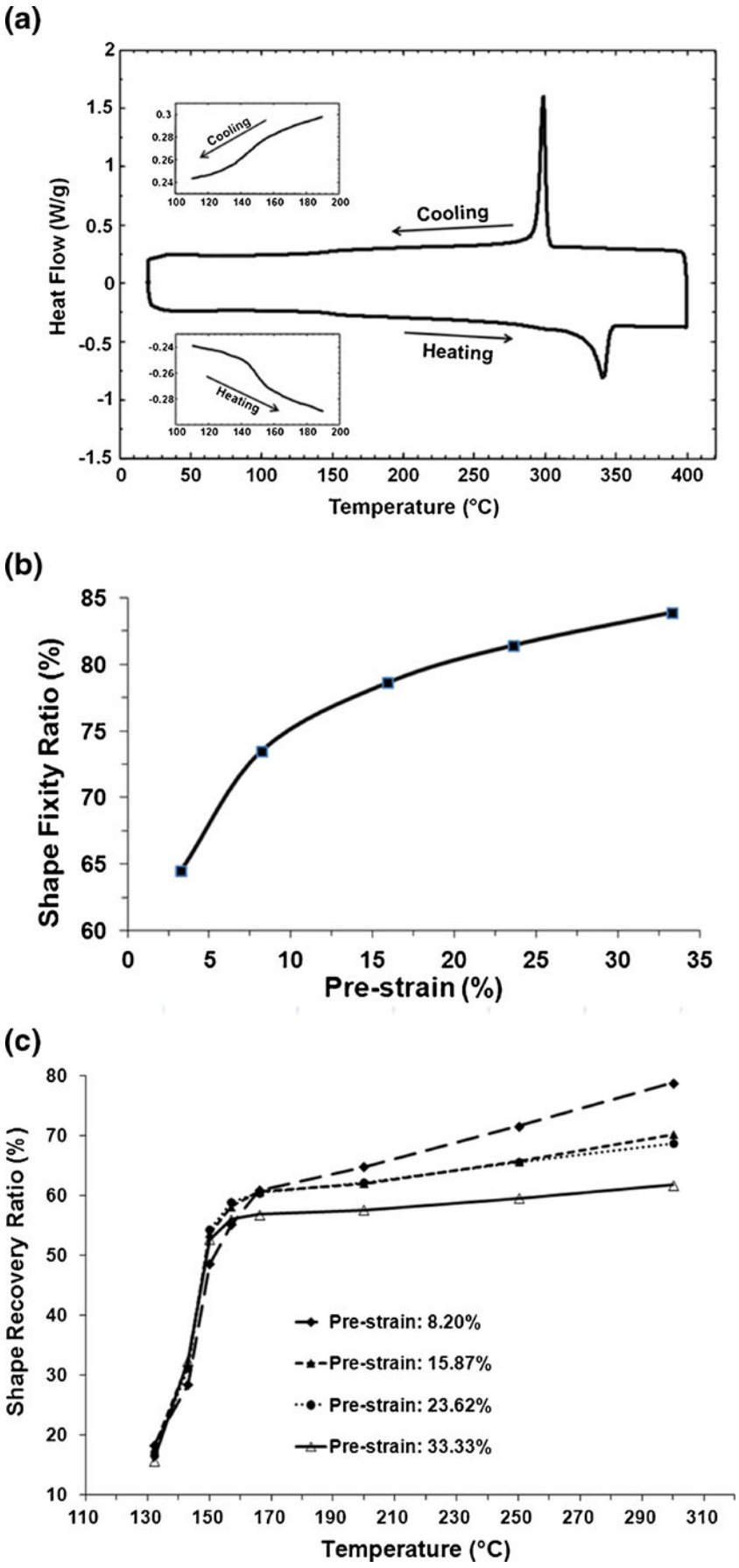

Fig. 22 The SME in a 0.1 mm thick PEEK film. **a** DSC result (at a heating/cooling rate of 10 °C/min). Insets: zoom-in views of the glass transition in heating/cooling; **b** relationships of shape fixity ratio vs. maximum pre-strain in programming; **c** evolution of shape recovery ratio upon heating

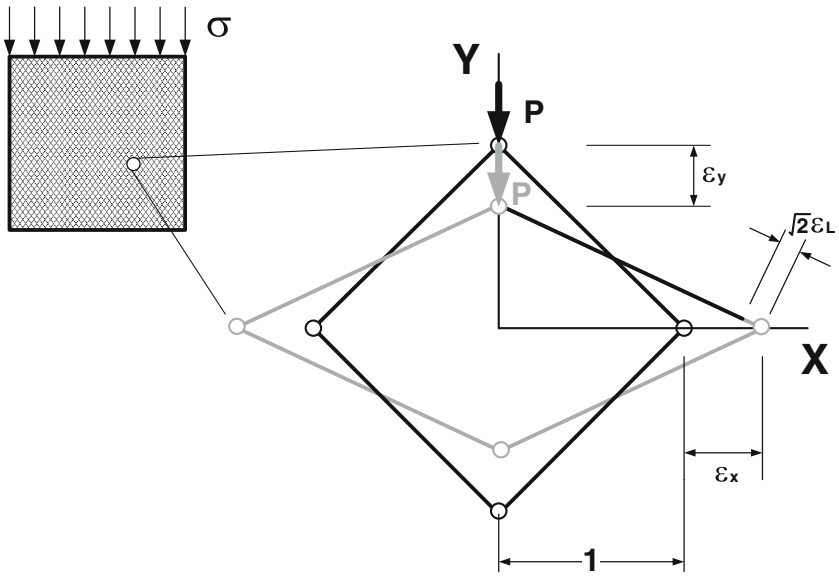

Fig. 23 Illustration of an elastic foam/network fully filled with transition component

recoverable strain) is achievable by using an elastic component with a higher elastic strain limit. For the purpose of reinforcement of a polymer as a structural material at its normal working conditions, we should load hard fillers only within the transition component in order to minimize the deterioration in the SME. In order to have a high actuation stress at above the transition temperature, we need to enhance the elastic modulus of the elastic component.

In addition, from Fig. 23 we may see that by utilizing the elasticity of the elastic network (yet softened transition component), the SME based on PTM can be realized. However, the exact achievable shape recovery ratio is very much dependent on the flexibility of the elastic network, and thus the programming temperature should be carefully selected.

Volume fraction of transition component

In the case that the SME is based on DCM or PTM, the volume fraction of the transition component/part directly or indirectly determines the flexibility of the elastic component/part and thus the shape fixity ratio and the shape recovery ratio, etc. Hence, we need to know the upper limit of the volume fraction of the transition component/part. For PTM, the volume fraction of the transition part can be roughly determined by the programming temperature. Certainly, temperature distribution is a key factor to ensure good SME. Hence, we must have the temperature variation within the material to be as small as possible.

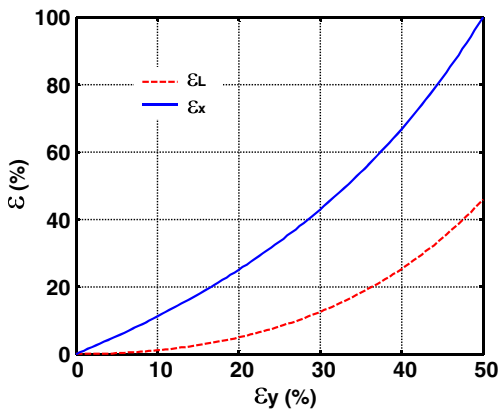

Fig. 24 ε_L and ε_x in terms of compression strain (ε_y)

Microscopically, the upper limit of the volume fraction of the transition component determines the continuity and density of the elastic network, which if being destroyed, reduces the shape recovery ratio. Transition component (inclusions) in a closed-cell form within an elastic component (matrix) is better than the transition component in an open-cell form in terms of preventing long distance flow of the transition component, which may cause damage to the elastic network at some weaker points, or may not be able to perfectly flow back during shape recovery (thus preventing full shape recovery).

In this section, from pure geometrical point of view, we consider the upper limit of the volume fraction of the transition component. Four ideal configurations are considered in Fig. 25a–d to represent well separated and uniformly distributed transition inclusions within a unit cell of elastic component (matrix). We may convert them into a standard equivalent morphology for easy comparison as shown in Fig. 25. Here, $2t$ stands for the minimal distance between two inclusions and D is the dimension of the unit cell.

In Fig. 25 (bottom), the relationships between volume fraction of inclusion vs. t/D are shown together for all four configurations. It is obvious that in all cases, at about 30 vol.% of inclusion, t/D approaches about 1/10, which indicates that the gap between inclusions is small so that

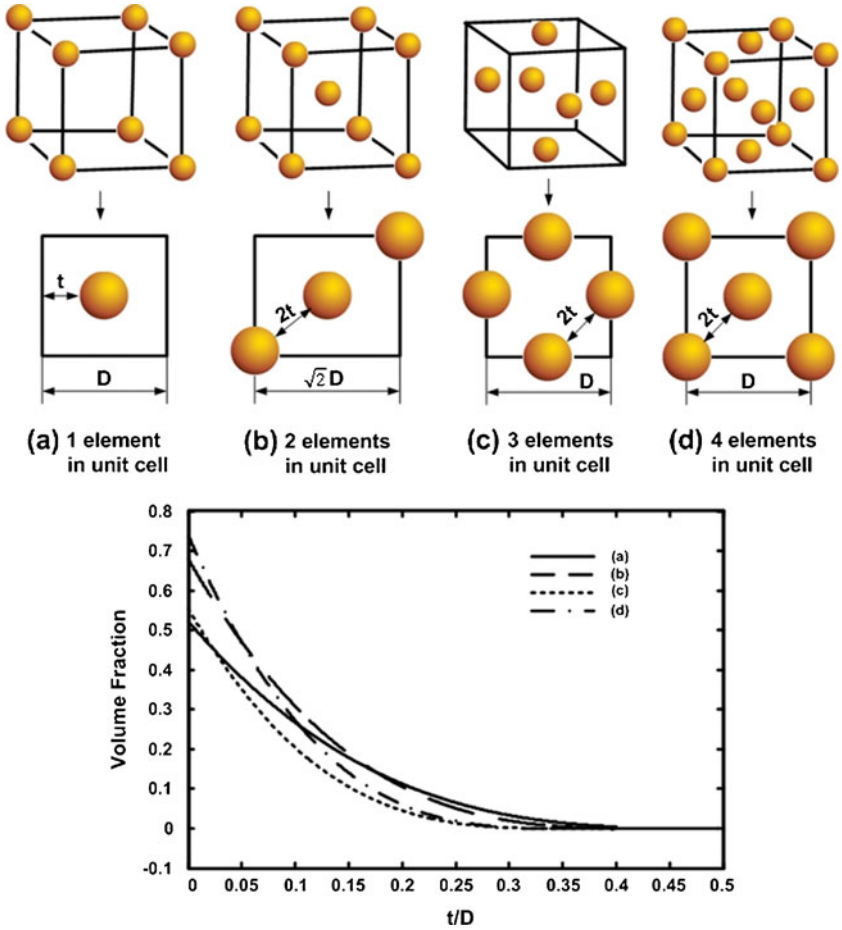

Fig. 25 Relationships between volume fraction of transition component vs. t/D

practically, we expect to see a number of open-cells. As such, the upper limit of the volume fraction of the transition component/part should be around 30 to 40 %.

The influence of the volume fraction of the transition component on the shape fixity ratio in silicone/paraffin wax (S/PW) hybrids (S-PW*x*, where *x* indicates the volume fraction of PW, ranging from 15 % to 40 %) programmed at above the transition temperature (melting temperature of PW) to different maximum compressive strains is presented in Fig. 26. This type of hybrid is selected as it has a very clear dual-domain structure (refer to Fig. 5 for its typical micro morphology), in which there is clearly no interaction between silicone and PW.

What presented in Fig. 26a is the shape fixity ratio vs. the volume fraction of PW curves at different maximum programming strains, from 5 % to 50 %. For easy visualization in comparison, in Fig. 26b, the results were re-plotted in terms of the shape fixity ratio against the maximum compressive strain. It is clear that with more PW content in a hybrid, shape fixity ratio increases monotonically. This

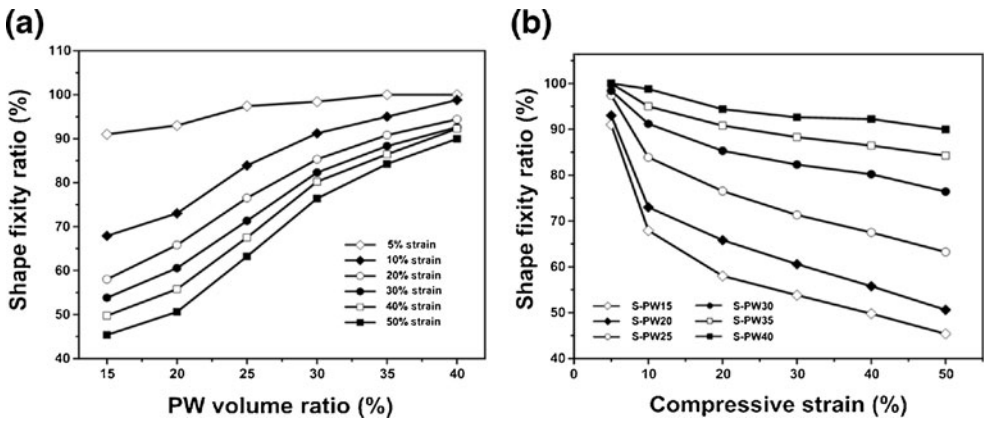

Fig. 26 **a** Shape fixity ratio vs. volume fraction of PW relationships at different maximum compressive strains; **b** shape fixity ratio vs. maximum compressive strain relationships

trend of increase is more significant at higher programming strains. It is also interesting to take note that the shape fixity ratio is actually higher at a smaller maximum programming strain in all samples. Surprisingly, this finding is consistent throughout all experiments, which may be due to that the applied load in programming is uniaxial compression, and engineering strain is applied in the analysis.

When comparing Fig. 22b (PEEK film in uniaxial tension) with Fig. 26b (S/PW hybrid in uniaxial compression), it is clear that the trend of shape fixity ratio vs. pre-strain curve may vary from one material to another.

Shape recovery progress

In a few recent investigations, it is both theoretically and experimentally proved that the programming temperature does have strong influence on the shape recovery progress upon heating [30, 52, 91, 139]. If the programming temperature is within the transition temperature range, in the subsequent heating process for shape recovery, a large portion of shape recovery occurs upon heating to around the previous programming temperature. By examining the instant strain recovery rate, Xie et al. [30] found that the maximum recovery rate is achieved at about the previous programming temperature. The underlying theory behind this phenomenon is schematically revealed by Sun et al. [91], which is actually based on the assumption of small programming strain (but not explicitly spelt out over there). Therefore, it is not able to match different types of shape recovery vs. heating temperature relationships in thermally induced recovery tests, in which the samples are programmed at different temperatures and to different maximum programming strains.

In Fig. 27, we assume the evolution of transition fraction upon heating follows the solid grey line. The transition start and finish points are denoted by T_s and T_f, respectively. If a polymer is programmed at high temperatures which are within T_s and T_f, but close toward T_f, the transition fraction

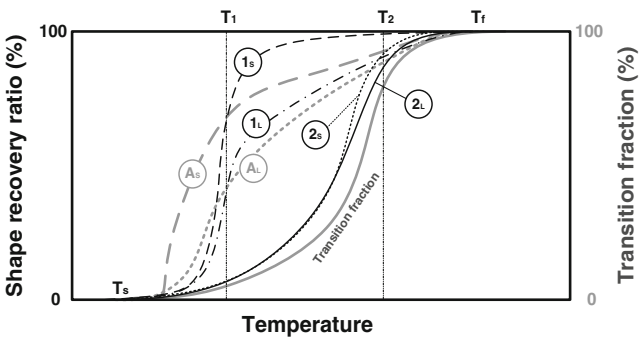

Fig. 27 Shape recovery ratio and transition fraction against heating temperature curves. A_S and A_L: recovery ratio upon heating to the programming temperature. Subscripts S and L denote small strain and large strain, respectively

is high and thus the softened transition component, which is relatively easy to *flow*, is in dominant. As such, whether it is a small or large programming strain, the targeted maximum programming strain, supposed to be within the strain limit, can be comfortably accommodated without evolving much quasi-plastic distortion in the non-softened portion of the transition component. Consequently, the shape recovery ratio vs. heating temperature curves for large programming strain (2_L, dark solid line in Fig. 27) and small programming strain (2_S, dark dotted line in Fig. 27) are about the same. In addition, we can see that by heating to the previous programming temperature, the original shape can be largely recovered.

For lower programming temperature cases, the evolution of shape recovery upon heating is programming strain dependent. For a small programming strain, the required deformation during programming can be largely accommodated by means of *flowing* of the softened portion of the transition component, elastic distortion in the elastic component, and elastic deformation (plus some slight quasi-plastic deformation) of the non-softened portion of the transition component. Consequently, the original shape can be largely recovered by heating to the programming temperature (1_S, dark dashed line in Fig. 27). At high programming strains, the non-softened portion of the transition component may be quasi-plastically distorted. Therefore, upon heating for recovery, shape recovery at around the programming temperature is remarkable, but is still partial. Further heating is required for further recovery in a gradual manner (1_L, dark dash-dotted line in Fig. 27).

We need to bear this in mind that in many applications, such as programmed active disassembly of obsolete electrical devices, in which we should program the parts, which are expected to drop out at lower temperatures, to lower strain only to ensure well controllable recovery in a more precise manner [140].

Now consider the influence of maximum strain on samples programmed at low temperatures. What reported in Fig. 22c is the evolution of shape recovery ratio upon heating to 300 °C, which is in its early melting stage (Fig. 22a), in four PEEK thin films pre-stretched to different maximum strains at room temperature. Remarkable shape recovery is observed upon heating from 130 °C to 165 °C, which is about its glass transition range (refer to the bottom inset in Fig. 22a). Shape recovery is over 50 % at 165 °C in all samples.

It is concluded that this PEEK thin film is not able to achieve full shape recovery (even after being heated to 300 °C and it turns warped). At 130 °C, all samples have already had over 10 % shape recovery, which might be the result of relaxation. Even shape recovery is partial, all shape recovery ratio vs. heating temperature curves up to 165 °C are virtually about the same. This is more or less expected, just like in those experiments, in which programming is conducted at

high temperatures (above transition range) (e.g., [109]). Since the transition component is distorted more or less uniformly, the recovery sequence should largely follow the transition fraction vs. heating temperature curve (solid grey line in Fig. 27) for any maximum strains in programming.

Further shape recovery is observed, but only slightly and gradually, upon gradually heating to 300 °C. More recovery is found in the less stretched sample.

Shape recovery ratio and multiple-transition

In the case of SMMs with perfect SME, following the above discussion in Section "Shape recovery progress", we can see that the shape recovery ratio upon heating to the previous programming temperature also depends on the maximum programming strain (Refer to Fig. 27). In the case of small programming strain, the shape recovery ratio vs. temperature (standing for both the programming temperature and heating temperature for shape recovery, as they are the same) relationships should follow the dashed grey line (A_S), while for a large programming strain, it should be closer to the dotted grey line (A_L). We expect to see complete or very close to 100 % shape recovery upon heating to or above the transition finish temperature. In the following discussion, our focus is on incomplete shape recovery.

To be more generic, our experiments were conducted using commercially available engineering polymers, which we do not have full knowledge of their exact chemical compositions. The applied standard programming procedure includes three steps: deforming at a specified temperature, cooling and then unloading. Again, we assume time-dependent parameters are negligible.

The SME in the biodegradable polymer presented in Fig. 21 was investigated. In the first step, the programmed samples were heated to their individual programming temperatures for 30 min. The resulted shape recovery ratios (as shown in Fig. 28) reveal that shape recovery in all samples is always incomplete. The general trend is also different from that mentioned in Fig. 27. More interestingly, the maximum shape recovery ratio occurs at about 60 °C, which is coincident with the peak transition temperature as shown in the DSC curve in Fig. 21.

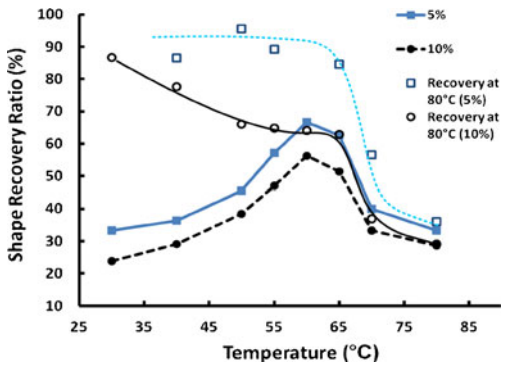

Fig. 28 Shape recovery ratio (recovered upon heating to the programming temperature and then to 80 °C) as a function of programming temperature at two different maximum programming strains (in uniaxial compression)

As previously discussed, a substantial amount of incomplete shape recovery, in particular at high programming/heating temperatures, indicates a significant amount of *plastic* deformation in the elastic component and/or non-reversible *flow* in the transition component. This is further confirmed by two more observations from Fig. 28, namely the higher the maximum programming strain is, the lesser the shape recovery ratio is; and the higher the programming temperature is, the lesser the shape recovery ratio is in the temperature regime close to the transition finish temperature. Previous discussions on the maximum strain in programming (Section "Maximum strain in programming") and volume fraction of transition component (Section "Volume fraction of transition component") provide the basic underlying mechanisms to explain the reasons behind this phenomenon.

A more obvious way to verify plastic deformation, if any, after programming, is to check the final shape recovery ratio after heating to above the transition range. In the second step, all samples were further heated to 80 °C, and the shape recovery ratios were recalculated and added into Fig. 28. The observed trend is different from the silicone-PW samples (Fig. 26), in which full shape recovery is always observed after heating to above the melting temperature of PW. In this biodegradable polymer, we can see a substantial amount of increase in shape recovery ratio in 5 % pre-strained samples programmed at temperatures lower than about 70 °C (note that this trend is almost identical to that reported in [141] (Fig. 5), in which the reported relationship is between the shape recovery ratio and the weight fraction of the transition component. From mechanism point of view, the weight fraction of the transition component and programming temperature are equivalent), while for 10 % strain cases, remarkable increase in shape recovery ratio only occurs in samples with a programming temperature lower than about 55 °C. Referring to Fig. 21b, we may conclude that the exact residual strain (rather than the maximum programming strain) should play an active role to influence the final shape recovery after heating to 80 °C. The strong interaction between the elastic and transition components during programming at low temperatures reduces the shape fixity ratio, but actually helps to reach a higher shape recovery ratio.

As revealed in Fig. 22c, the PEEK films are able to have some slight further shape recovery upon further heating before warped at near its melting temperature. The less stretched sample is able to recover more. The final shape recovery ratio is over 75 % in the sample with a maximum pre-strain of 8.2 % (about 15 % increase upon further heating from 160 °C to 300 °C), while for the sample pre-

stretched to 33.33 %, the final shape recovery ratio is about 60 % (the increase upon further heating from 160 °C to 300 °C is only around 5 %). It seems that there is a possibility to reach even higher recovery by further heating over another transition range, provided that the polymer is still able to keep its shape.

In another set of experiments, a polytetrafluoroethylene (PTFE) ring (from Woer Heat-shrinkable Materials Co., Ltd., Shenzhen, China) was tested for its SME. DSC result of this polymer is shown in Fig. 29, in which we can see a clear melting transition at over 300 °C. However, melting and solidification emerge at two slightly different temperature ranges, which indicates the nature of hysteresis in this polymer in this transition. A close-look reveals that the temperature range for glass transition is from about 100 °C to 120 °C (Fig. 29, insets). It should be pointed out that the PTFE is still intact even after being heated to 340 °C, which is over the melting temperature range.

A similar set of SME tests (as conducted in the above mentioned biodegradable polymer in Fig. 28) were carried out on the PTFE rings (refer to Fig. 30b for the dimensions of the ring sample). They were programmed at three different temperatures (all within the glass transition range). But instead of uniaxial compression, they were expanded to a maximum expansion of 50 %. Figure 30a reveals a similar trend in the shape recovery ratio vs. programming temperature relationships as that in Fig. 28 (upon heating to the programming temperature).

In a further test on the same type of PTFE ring, we increased the amount of expansion to 80 % and the programming temperature to 120 °C. After heating to 120 °C for shape recovery, the measured shape recovery ratio was 37 %, which is lower than all the previously obtained ratios (refer to Fig. 30a). Seemingly more plastic deformation was developed in this ring. However, upon heating gradually to 340 °C, which is over the melting transition range of this polymer, eventually, 100 % shape recovery was achieved. Same shape

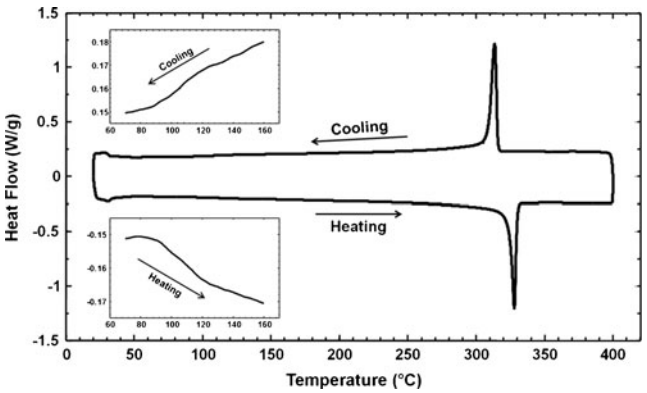

Fig. 29 DSC result of PTFE (conducted at a heating/cooling rate of 10 °C/min). *Inset*: zoom-in views of the glass transition range upon heating and cooling

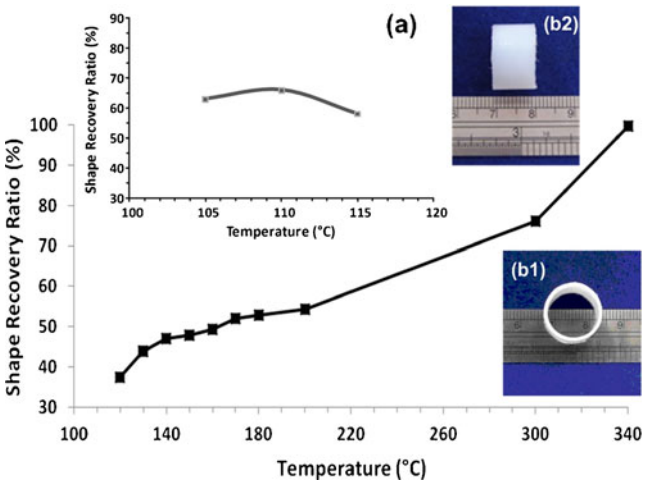

Fig. 30 Evolution of shape recovery ratio against heating temperature in a PTFE ring (80 % maximum expansion at 120 °C in programming). **a** Shape recovery ratio vs. programming temperature relationships upon heating to the programming temperature (50 % maximum expansion in programming). **b** Photographs of the PTFE ring before testing

recovery ratio trend (i.e., full recovery upon gradually heating to 340 °C) was observed in all tested rings under all programming conditions. In addition, this phenomenon (i.e., further heating to reach full recovery) was also observed in another set of experiments carried out on 0.1 mm thick PTFE films.

It is clear that for PTFE, the non-recoverable deformation upon heating to over the glass transition temperature range is actually fully recoverable by means of further heating to above the melting transition temperature. It seems that within the glass transition range, the *transition* component (T_1)-*elastic* component (E_1) system is able to achieve higher shape recovery ratio, only if the applied strain is small. Under high programming strains, E_1 is further decomposed into two parts, namely elastic component (E_2) and transition component (T_2). Heating to soften T_1 is not good enough for full shape recovery. Only by heating to above the softening temperature of T_2, full shape recovery can be obtained. The above mentioned observation that at 340 °C, which is above the melting temperature range, the PTFE is still intact is a good evidence to prove the existence of E_2.

Further discussions

Normally, it is not easy to introduce a new material into an industry, particularly in the field of biomedical engineering. Using existing material is a short-cut to avoid many difficulties and to shorten the journey of R&D. A couple of examples are presented here to demonstrate how to utilize the SME in engineering polymers for new functions.

PETG, glycol-modified polyethylene terephthalate, is a copolyester and transparent. It has high stiffness, hardness,

and toughness as well as good impact strength. PETG is a commonly used material for transparency. Instead of using PU as reported in Huang et al. [29], PETG sheet, which is available off the shelf in almost any stationery shops, can be used as refreshable Braille paper for people with vision problem to easily remove any typographical errors by means of thermally induced shape recovery and retype just like writing with a pencil and eraser (Fig. 31).

Due to its convenience, in particular in minimally invasive surgery, surgical stapler has become a widely used tool to replace (at least partially) surgical suture. Biodegradable staples are preferred so that the staples disappear after a few months, and thus a second operation to remove the staples becomes unnecessary. However, unlike sutures which are able to be tightened to close the wound, staples are lacking in this tightening function. Hence, as normally suggested, a wound should be closed using a forceps before firing a surgical stapler. After programming a commercial PLA based staple, which is biodegradable, as revealed in Fig. 32, the staple has the ability to close the wound automatically by means of the thermally induced SME. Unlike SMAs [65], the force generated by the SME in polymers is normally only a few MPa or less [29, 66, 109], which is compatible to human tissue, and also adjustable. The problem of over-stressing, which may prevent good blood circulation and cause damage to tissue, can be avoided. In addition, at present, different sized staples are required for tissue with different thicknesses. The shape recovery ability in polymer staples can be utilized to effectively reduce the number of staple sizes to one only.

EVA is biocompatible and has excellent elasticity. Traditionally, EVA is used for drug delivery devices in biomedical engineering applications. A temporary stent (such as for the treatment of prostate cancer) made of EVA in a flower-shape (Fig. 33a), may be eluted with drug, can be expanded into a big circular shape (Fig. 33b) and then elastically deployed at the required location. Drug is able to be released gradually to prevent infection, thrombosis or other problems. After the period of treatment is over, the EVA stent is heated and it shrinks back into its original flower-shape (Fig. 33c), so that one can easily remove it. As an alternative, as proposed in [90], we may use the drug as the transition component. After the drug is released, the stent shrinks automatically.

The SME in polymers is applicable not only to devices for actuation or controllable motion generation, but also as an advanced manufacturing technology. The thermo-responsive SME and chemo-responsive SME can be used either individually or together.

The SME has been applied for instant micro patterning atop a PS SMP over a large area in a cost-effective manner (Fig. 34a). Microlens array, which is required in many applications, for instance, in a recently emerging field of light field microscopy to achieve, so called "Shoot first, focus later" [142], can be produced atop PMMA, which is a conventional optical polymer, utilizing the SME. One step further, Fig. 34b presents a microlens array atop a cylindrical PMMA lens, which is to mimic "insect eyes" for a very large field-of-view and effectively tracking motion of objects [143, 144].

As mentioned above, for some polymers, we may chemically tailor their transition temperatures to around the required

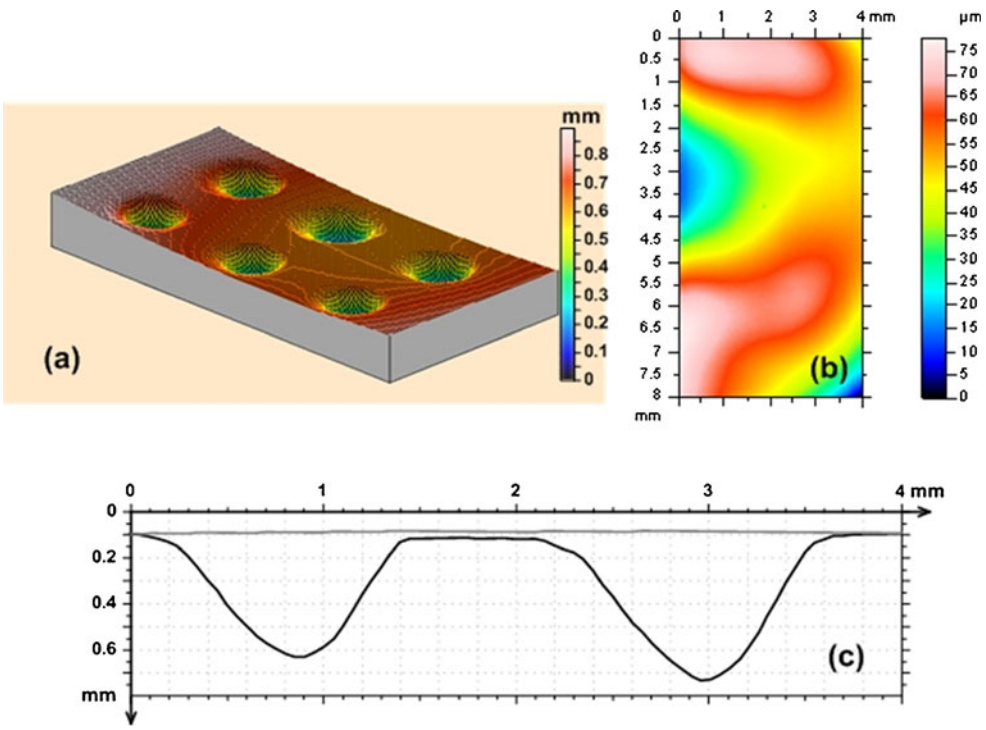

Fig. 31 PETG refreshable Braille paper. **a** After indentation (three-dimensional view); **b** after heating to 75 °C for shape recovery; **c** comparison of cross-sections (*black line*: after indentation; *grey line*: after recovery)

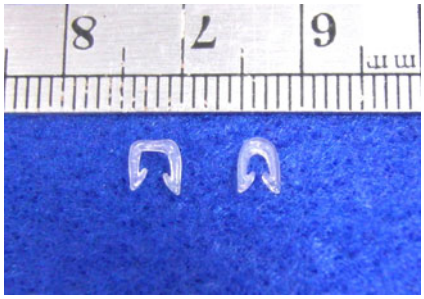

Fig. 32 The SME in a commercial biodegradable PLA based staple. *Left*: after programming; *right*: after heating

temperature range which is required in a particular application, and then by means of selecting the programming temperature to fine-tune the shape recovery temperature. This could be an alternative to chemical composition tuning to modify the transition temperatures (e.g., [145, 146]).

Some major issues on the fundamentals and optimization of the shape memory performance have been discussed in details in Section "Fundamentals and optimization of the SME". This section focuses on the concerns in the actual implementation.

Influence of processing and pre-heat treatment

Some commercial engineering polymers are processed in such a way that they may be sensitive to further heat treatment. For instance, thin PMMA sheets may contract a few percent upon annealing; while for PMMA rods, heating to around their melting temperature may induce bubbles all over the material. In addition, pre-heat treatment may alter the transition(s). As shown in Fig. 35, in the first heating process, we can see two transitions, one is glass transition and the other is melting transition. However, in the follow-up second heating process, there is no melting trough and the glass transition temperature range is also lower. Consequently we need to determine the programming parameters according to the exact conditions of a polymer.

Theoretically, programming can be carried out during either heating process or cooling process. As discussed in Sections "Volume fraction of transition component", "Shape recovery progress" and "Shape recovery ratio and multiple-transition", the key factor, which affects the SME, is the volume fraction of the softened part of the transition component. Hysteresis can be found in many polymers (e.g., in Fig. 29 in a PTFE during melting). We need to pay attention to all these factors in the determination of the processing/programming procedure and parameters.

Multiple-SME

Instead of returning to the original shape directly (called as the dual-SME, since there are only two stable shapes involved, namely the temporary shape, i.e., the shape after programming, and the original shape, i.e., the permanent shape), it is a great advantage if we can have one or more stable intermediate shapes between the temporary shape and the original shape, so called the triple-SME (with one intermediate) and multiple-SME (with multiple intermediate shapes), so that we can program a polymer to work as a machine, i.e. "The material is the machine" [147].

One possible approach is to introduce a gradient transition temperature [111, 148]. As shown in Fig. 36, a piece of PU SMP wire is able to recover its original straight shape in two steps upon immersing into room temperature water (chemo-responsive SME). Since the top half of the wire has been immersed into the water to reduce the T_g, this part straightens first.

If there are two transitions in a polymer, which have remarkably different transition temperature ranges, we may stretch the polymer at either high or low temperatures for programming. Subsequently, upon heating we may see two significant contraction events. Each of them corresponds to one transition temperature range. This programming approach is simple, but only applicable when the modes of both shape recovery are the same (e.g., all in tension or contraction), and lacks flexibility to control the magnitude in each shape recovery event [149].

A more practical approach so that the shape recovery can follow any prescribed sequence and in any mode/magnitude, is to program in a step-by-step manner. Previous experiments showing the multiple-SME require the SMPs to have two or more transitions, so that each transition corresponds to one shape [150–154]. In the case of the triple-SME, in addition to synthesize/modify a polymer with two transition components, which have two well separated different transition temperatures, the glass transition and melting transition are naturally

Fig. 33 EVA stent. **a** Original shape; **b** after programming; **c** after shape recovery

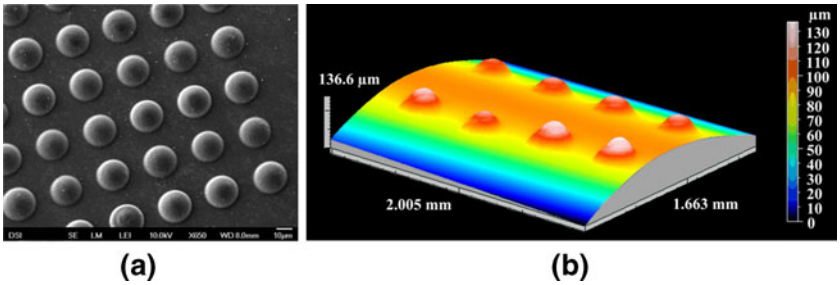

Fig. 34 Cost-effective surface patterning over a large area using laser for thermally induced shape recovery (**a**) and compound microlens array (*insect eyes*) fabrication using both thermally and chemically induced shape recovery (**b**). **a** is reproduced with permission from IOP Publishing [93]

available for many polymers to utilize. An extreme situation is to have a bilayered structure with different transition temperature in each layer [155, 156].

What Xie T [157] has demonstrated is to achieve the multiple-SME in a polymer within one single transition, which has a wider transition temperature range. If we program a polymer step by step at a few different temperatures (within the temperature range of a transition) during cooling, the transition component is hardened in a step-by-step manner as well. Consequently, upon gradually heating, shape recovery in the polymer appears to be step-by-step accordingly, but following a reverse order as that in programming [158].

Since the glass transition temperature range of most polymers is over 20 °C, the glass transition should be good enough for at least the triple-SME (e.g., one programming temperature is above T_g, one is below T_g, as shown in Fig. 37).

Ideally, if the transformation progress in both heating and cooling follows a same particular function against temperature, the programming temperature(s) and heating temperature(s) have a clear one to one relationship, i.e., a shape distortion fixed at a particular temperature is going to be recovered by heating to this temperature again. However, according to Fig. 27, we need to ensure that during programming, the distortion in the subsequent step(s) should not destroy the previously programmed shape(s). Hence, the magnitudes of the applied distortion in a series of programming steps upon cooling are suggested to follow a decreasing order. In some occasions, we may heat slightly above the corresponding programming temperature to have better shape recovery in this heating step (Fig. 38).

As a particular case, a piece of silicone beam filled with paraffin wax is able to bend downward and then upward upon immersing into hot water (with a constant temperature) [66]. Of course, the down-and-up motion is due to gradual temperature increase.

The triple-SME may be used in both deployment and retraction of polymer stents, all by means of minimally invasive surgery [29, 159]. Heating to about the same temperature twice for both deployment and retraction can be realized based on, for instance, moisture-induced T_g reduction [29] (refer to Fig. 13 for a typical example of moisture induced T_g reduction in PU SMP).

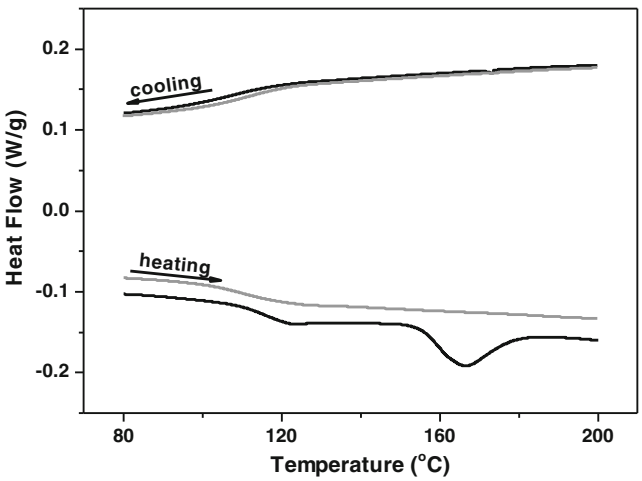

Fig. 35 DSC curves of a PMMA in two continuous thermal cycles at a constant heating/cooling rate of 5 °C/min. *Black line*: first cycle; *grey line*: second cycle

Temperature memory effect (TME)

The term of temperature memory effect (TME) is seemingly new to the SMP community. To researchers within the field

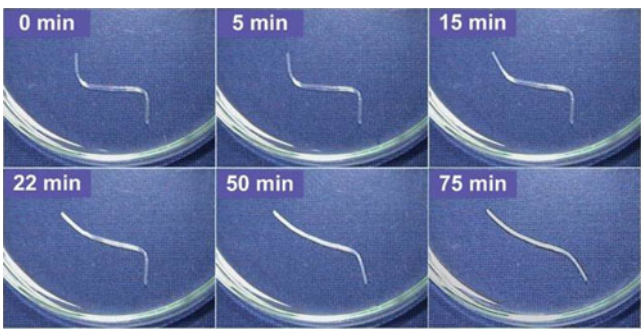

Fig. 36 The triple-SME in a PU SMP wire upon immersing into room temperature water. Reproduced with permission from American Institute of Physics [111]

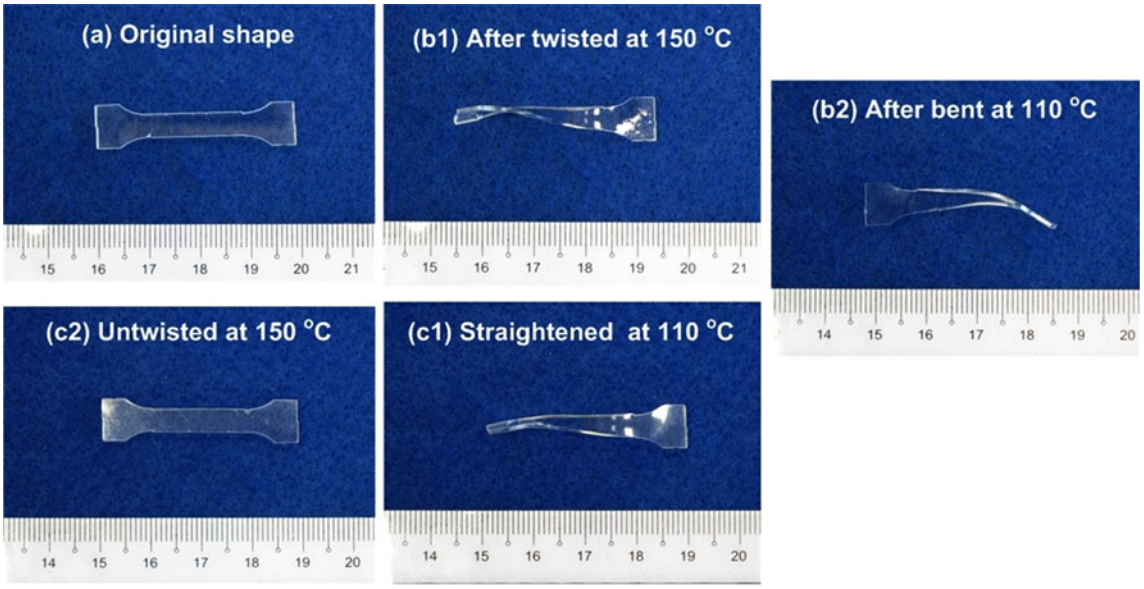

Fig. 37 Triple-SME in PMMA. **a** Original shape; **b** programming during step-by-step cooling; **c** shape recovery during step-by-step heating

of SMAs, the metallic counterpart of SMPs, the TME (or in some other different names in early days) is a phenomenon which has been subjected to intensive investigation for a few decades [160–162]. It refers to the ability of a material to reveal the previous maximum heating temperature(s) (provided it is within the phase transformation temperature range) in the following heating process. In the case of multiple heating cycles, if the maximum heating temperatures in thermal cycling follow a decreasing order, in the last heating process, all the previous maximum heating temperatures can be spotted from, for example the result of DSC test [163]. Now, the TME is considered to be a generic phenomenon in many SMAs in various types of phase transformations. Although still lacking in experimental observation to provide direct and un-doubtable evidence, different martensite variants produced during thermal cycling, which undergo transition in a step-by-step manner upon heating, are believed to be the reason, which has been indirectly proved by the result of DSC test [164].

Probably, [165] is the first paper explicitly revealing the TME in a polymeric material, followed by [157] in which Nafion, which also have a wide transition temperature range as the polymeric material tested in [165], is the polymer subjected to investigation. Since then the TME in SMPs started to attract great attention [30, 139], and its fundamental mechanism has been sketched in [158] (a revised version is reported in [29]).

Although the TME in SMPs is normally observed in so called constrained recovery test (i.e., heating for shape recovery with the programmed shape fixed, which is opposite to free recovery test in which constraint is fully removed before heating), which is a different type of experiment as

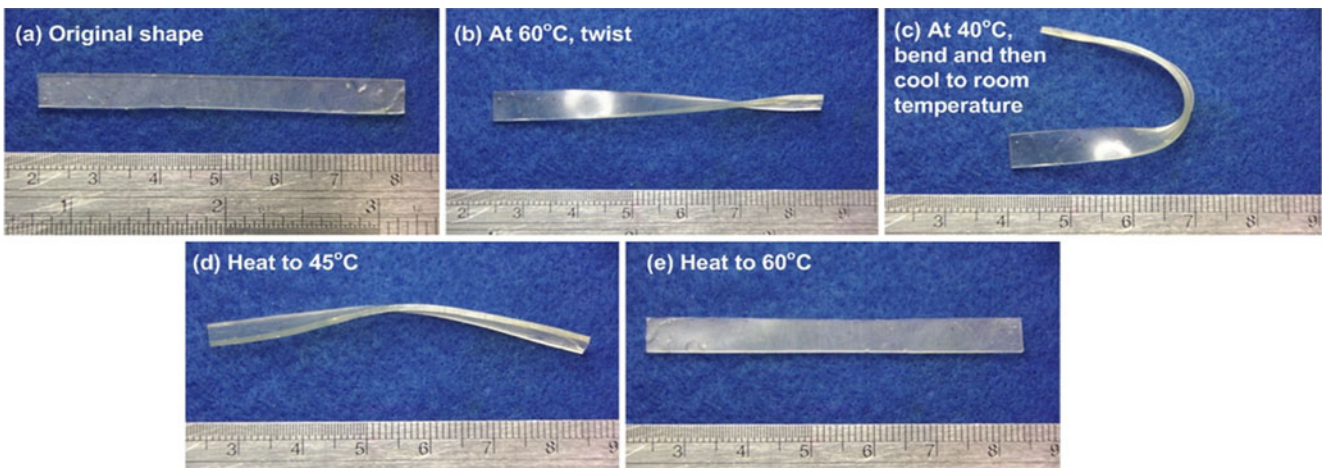

Fig. 38 Triple-SME in PU. In (**d**), the sample is heated to 45 °C (instead of 40 °C in (**c**))

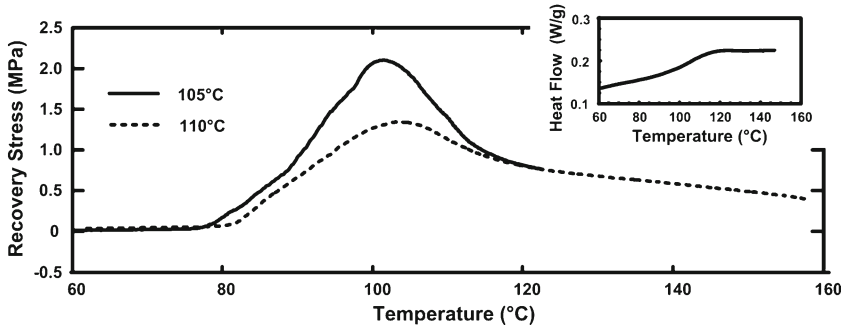

Fig. 39 The TME in PMMA. Samples were pre-stretched to 100 % at a strain rate of 0.001/s at 105 °C and 110 °C, respectively. *Inset*: DSC curve during heating (heating rate: 10 °C/min)

compared with the one normally used in SMAs, the underlying mechanisms for the TMEs in both SMPs and SMAs actually share a common feature. They are all due to step-by-step transition [158, 164]. Hence, referring to Fig. 27, it is not a surprise to see that upon gradually heating, the maximum shape recovery speed (i.e., derivative of recovery ratio with respect to temperature) may be observed at around the previous programming temperature in free recovery test [30]. On the other hand, it is obvious that the multiple-TME can be observed in a polymer after being programmed for the multiple-SME, since basically both phenomena have the same mechanism origin.

In a standard constrained recovery test, a programmed polymer is fully unloaded before being heated with the temporary shape fixed. We can observe a force/stress peak upon gradually heating. This peak is normally very close to the previous programming temperature, i.e., it is seemingly that the polymer is able to memorize the previous heating temperature, provided that the programming temperature is within the transition temperature range (e.g., in Fig. 39). This is where the term "temperature memory effect" comes from.

Apparently, apart from the testing conditions, e.g., precise thermal control (heating/cooling rate, temperature uniformity, etc), pre-stress etc, material's own properties, e.g., thermal expansion coefficient, softening procedure, and thermo-mechanical behaviors during transition, also play an important role on the exact location of the peak temperature.

In addition to the SME as presented in Fig. 7, Fig. 40 reveals the TME in melting glue and paraffin wax (again, based on the melting transitions in both materials). The programming temperatures are indicated. Since there are two peaks (one minor peak followed by a major peak upon heating) in paraffin wax, the recovery stress vs. heating temperature curves are more complicated as compared with

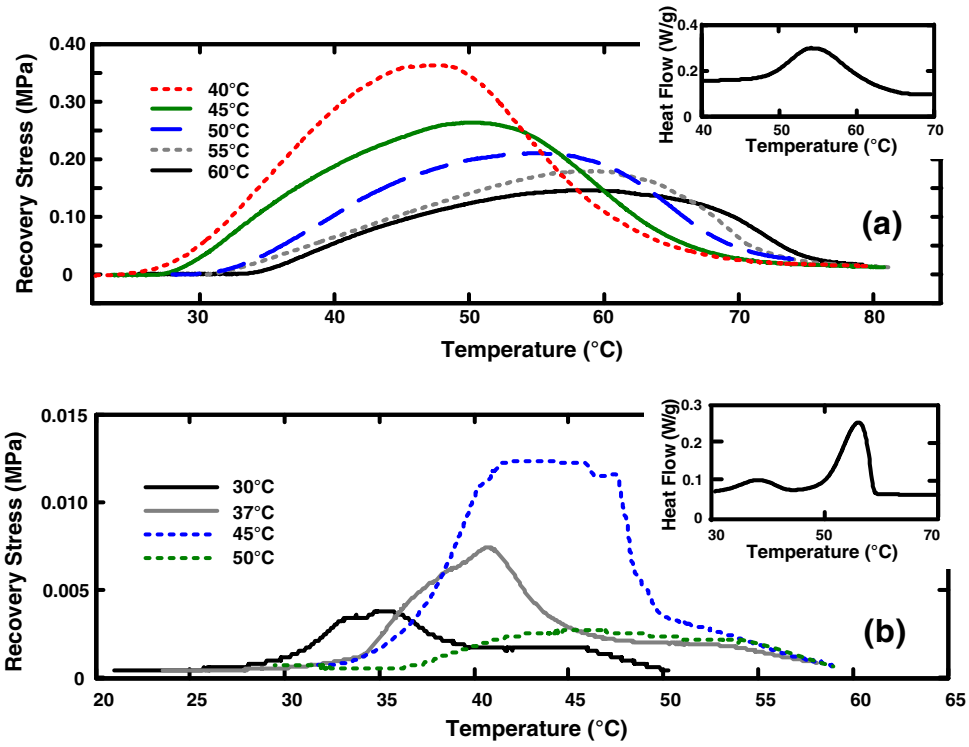

Fig. 40 The TME in (**a**) melting glue and (**b**) paraffin wax. The applied maximum strains (engineering compressive strain) were 30 % for melting glue and 50 % for paraffin wax. Applied strain rate: 0.001 s^{-1}. Insets: heating curve of DSC result (heating rate: 10 °C/min)

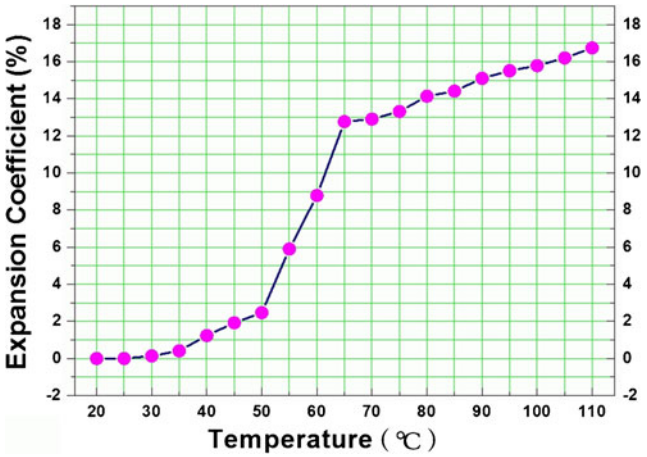

Fig. 41 Thermal expansion coefficient vs. temperature relationship of paraffin wax upon heating at a very slow speed

those of melting glue. Additionally, paraffin wax expands significantly upon heating (Fig. 41) and it melts into water-like liquid form at high temperatures. Therefore, unlike melting glue, which is still relatively highly viscous even it is fully melted, the stress peaks in paraffin wax programmed at different temperatures do not always occur at a temperature, which has a fixed temperature difference compared to the programming temperature.

As shown in [91], by optimizing the programming temperature, the maximum stress (together with other key performance parameters) in the TME (and the SME) can be adjusted. This adjustable maximum recovery stress is based on the mechanism which utilizes the hard portion of transition component (which does not go through the transition during programming) as the reinforcement to the elastic component, so that more elastic energy is stored in the polymer. Consequently, a recovery stress, which is higher than what the elastic component alone can provide, is observed. Before reaching the maximum stress, upon heating, the elastic energy stored in the polymer is released, so that the recovery stress increases continuously. After reaching the maximum stress, the hard portion of the transition component starts to soften (and thus collapses, which only happens at around the previous programming temperature), and therefore, the recovery stress starts to drop. As we can see, essentially this is due to the PTM.

SME in gel, protein and DNA

Polymer gels are able to dramatically change their volume in response to the change of an external factor, such as solvent, temperature, electrical field and light etc [121, 166–171]. As such, as demonstrated in Fig. 42, a silicone strip with hydrogel embedded in one side (only a part within the whole length of the silicone strip) is able to bend significantly upon immersing into room temperature water, and then to return to its original straight shape by means of drying. In addition, Fig. 43 reveals the feasibility to achieve wetting for shrinkage in a straw with a spherical hydrogel embedded inside [172]. The swelling of the hydrogel causes the length of the straw (with cuts) to decrease. Essentially, the SCE is utilized in the above applications.

Probably the first reported experiment to reveal the thermally induced SME in hydrogels was in [173]. As mentioned in [174], that copolymer gel, which does not show the SME in dry state, is able to have the thermo-responsive SME after being wetted in the water. However, according

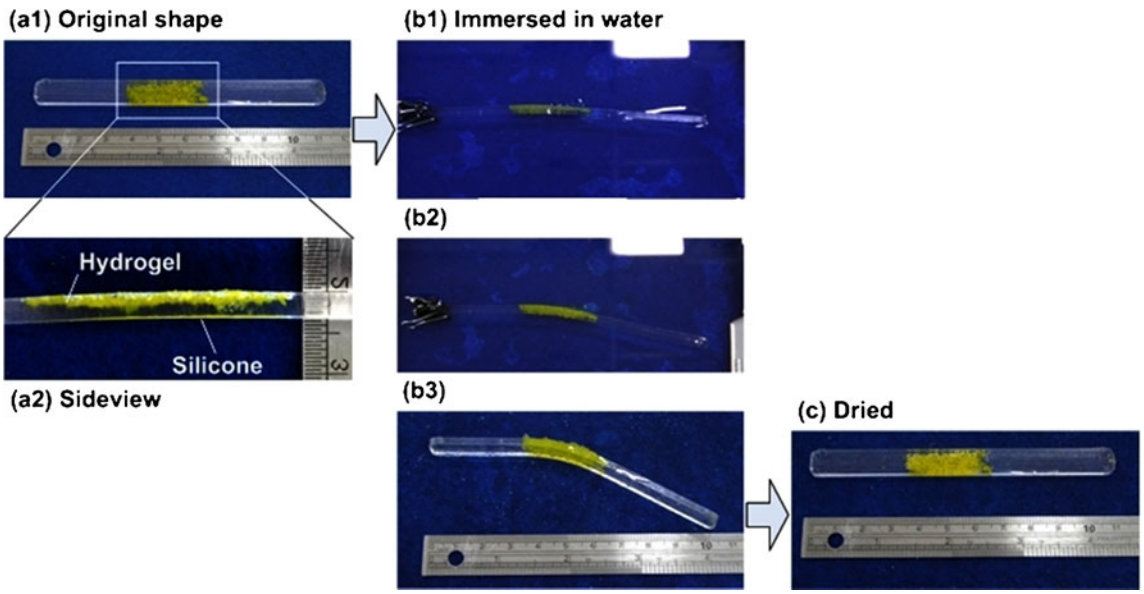

Fig. 42 Water induced SCE in a silicone strip with hydrogel embedded in part of it. **a** Original straight shape; **b** bending upon immersing into room temperature water; **c** shape recovery after drying

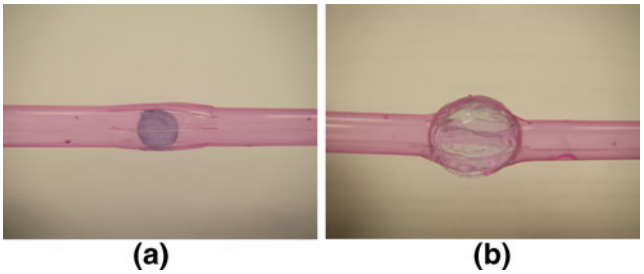

Fig. 43 Swelling of a spherical hydrogel inside a straw (with some local cuts). **a** Half-way wetted; **b** fully wetted. Reproduced with permission from VSP, an imprint of Brill [172]

to Fig. 44, a spherical hydrogel (Fig. 44a), which has been pre-compressed at high temperatures, is able to instantly and fully recover its original shape upon heating (Fig. 44b). On the other hand, pre-compressed hydrogels (being compressed at both high and low temperatures) are also able to gradually recover their spherical shape when placed inside an environment with a humidity level of 54 % (Fig. 44c), while inside an environment with 35 % humidity they fail to show any shape recovery at all even after 4 months (Fig. 44d). Previously, pseudo-elasticity has been observed in double network gels. Partial fracture of one network is believed to be the cause of this phenomenon [175], known as the Mullins effect [176]. However, we found that in partially wetted gels (by means of leaving them inside a chamber with high humidity level, e.g., 54 %), in which no obvious swelling was observed, they were able to viscous-elastically recover their original shape without any apparent damage at all.

In [35], along with glassy polymers, crystallisable polymers, polymer blends and filled polymer composites, polymer gels are regarded as an independent category, in which the formation of crystalline aggregates between the side chains is considered as the fundamental mechanism behind the SME. Above experiments reported in Fig. 44 reveal that there is nothing special in the polymer gels at all. Like ordinary polymers, they have both the thermo- and chemo-responsive features, in which the crosslinked polymer network serves perfectly as the elastic component.

In recent years, environment-sensitive gels have found many applications in biomedical devices and drug delivery [118, 119, 122, 123, 177]. In addition, degradable SMPs have been investigated for controlled drug release [18, 99–101, 178]. PEG is a water soluble polyether compound with many applications, in particular for medicine (e.g., in [179–181]). However, it is normally very much brittle and fragile, so that it is difficult to achieve apparent SME with a high recoverable strain. In Fig. 45, a hydrogel was placed inside PEG water solution and then dried to get rid of redundant water. The resultant hydrogel/PEG hybrid (wt% of PEG is 97.5 %) is stiff and has excellent SME, since the hydrogel serves both as the network to reduce the brittleness of PEG and as the elastic component for the SME. As the content of hydrogel is only 2.5 wt.%, this experiment successfully demonstrates an alternative approach to modify the mechanical and shape memory properties of PEG.

As reported, potato starch, which is carbohydrate $[C_m(H_{10}O_5)_n]$ produced by all green plants as a way to store energy, is both thermo-responsive and moisture-responsive [36]; maize flour also has excellent shape recovery capability upon heating [182].

Our recently obtained experimental results reveal excellent thermo-/moisture- responsive SME in human nail, which is made of translucent keratin (fibrous structural protein), a product of amino acids, which are also key elements of hair, horn, wool and silk etc (Fig. 46). It is not a surprise since protein and even DNA are essentially polymers as well, and therefore, they are harmless SMPs to environment. Excellent biocompatible and even biodegradable features make them suitable for

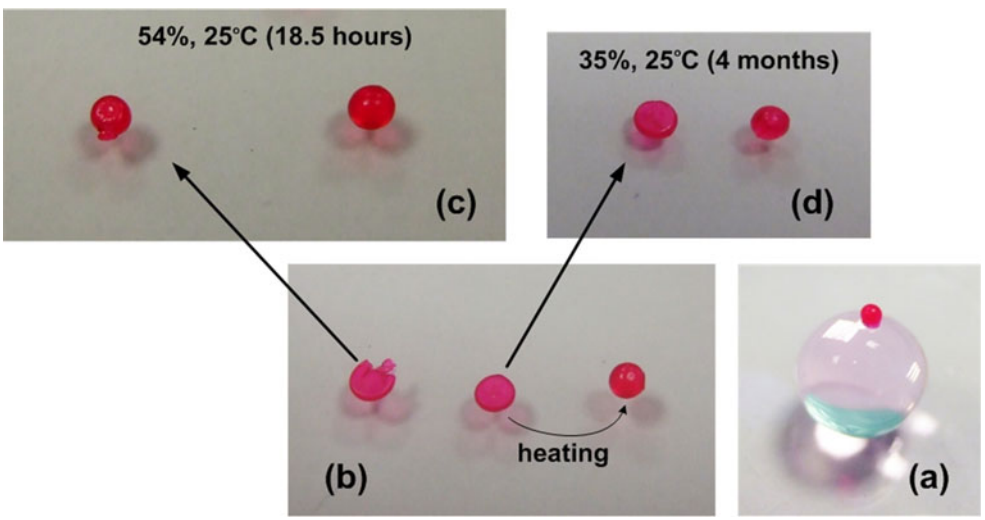

Fig. 44 Thermo- and moisture-responsive SME in a hydrogel

Fig. 45 Thermally induced SME in a hydrogel/PEG hybrid. **a** Original shape; **b** after being compressed at 100 °C; **b** after heating to 100 °C for shape recovery

many biomedical applications. One possible application is for the development of DNA based SMP, which is based on DNA folding/unfolding for surgery inside cells or targeted drug release.

Durability/stability

For simplification, in the above discussion, all time dependent parameters are ignored. It is well known that polymers are viscous and most of them are prone to stress induced relaxation and creeping. Hence, the durability/stability of the SME in polymers has turned out to be a major concern in many real engineering applications.

Although still very much limited, experimental investigation on the durability/stability of the SME of some polymers (including some engineering polymers) have been reported in the literature [22, 35, 183–189]. According to Hussein and Harrison [22], excellent shape recovery (over 90 % shape recovery) has been observed in polyethylene terephthalate (PET), ABS, PC, and their blends (ABS/PC) even after an elapsed time of two years after being programmed. This sounds promising, but needs further extension in the testing time in order for real engineering applications of engineering polymers for active disassembly of obsolete electrical devices.

It is expected that by means of careful selection of materials/processing method and design, the durability of the SME should be about the same as the durability of the original materials. In fact, the concept of dual-domain mechanism may provide an easy solution to estimate the durability/stability of the SME in a polymer based on the durability/stability of individual domain material.

Design and programming polymeric materials with tailored features

Novel SMPs with some special functions have been developed. A very interesting example of such is the SMP reported in [190], which has the built-in threshold temperature sensing function by means of color change during the process of the thermally induced shape recovery.

The dual-component concept (DCM) can be extended into the design of polymeric materials with tailored features. For instance, based on a similar working principle as the Mullins effect [176], pressure-responsive SMMs has been developed [23]. By introducing a transition component, which softens upon cooling (for example, Poloxamer 407 [191]), cooling-responsive SMMs can be made and the SME can be even achieved at around human body temperature [192]. A melting adhesive material can be used as the transition component to achieve thermal-assisted self-healing for simultaneous shape and strength recovery, which is beyond the healing of scratches on the top surface of a polymer by means of shape recovery only [23, 66, 103, 193]. As an extreme case, if water is used as the transition component, we will then be able to achieve a very sharp transition range in a SMM (at ±0 °C) [23]. On the other hand, as an extension of the concept of the multiple-SME, we can achieve tailored transition temperature within the specified range by programming.

We may develop polymers with a few different transition components, which are responsive to different chemicals or different types of stimuli (e.g., heat, chemical or light), so that each recovery motion can be controlled independently. Remote controlled multi-shape polymer nanocomposites with selective radiofrequency actuations have been invented [154].

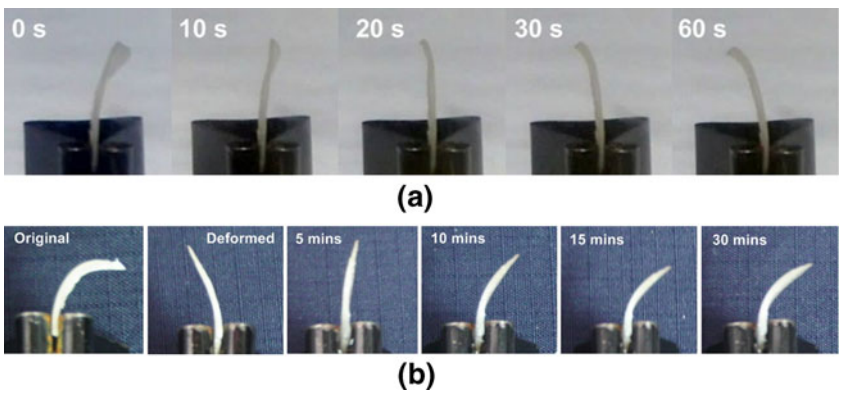

Fig. 46 The SME in a human nail. **a** Upon heating inside 65 °C hot chamber (thermo-responsive); **b** upon immersing into 22 °C water (chemo-responsive)

Conclusions

As we can see, polymers (including their composites/hybrids and other non-conventional polymers, such as protein and DNA etc) are intrinsically with the thermo- and chemo- responsive SME. As such, the SME should essentially be a material property, just like density and specific heat, of all polymers. Hence, without introducing any new material (and even without any material modification), utilizing the thermo- responsive SME and chemo- responsive SME of an existing polymer, either individually or combined together, we can come out with many approaches to reshape device/product design and to develop new fabrication techniques.

On the other hand, in addition to blending and varying chemical composites and/or synthesis process, the SME of a given polymer can be optimized by means of selecting the right programming parameters only.

Based on the fundamental mechanical mechanisms of the SME, we can also design and develop new polymeric SMMs with tailored features and performance.

Acknowledgments LW Lim, MY Jiang and SM Shee helped to conduct the experiments reported in Fig. 13, Figs. 28 and 31, respectively. The PTFE reported in Figs. 29 and 30 was kindly provided by Woer Heat-shrinkable Materials Co., Ltd., Shenzhen, PR China.

References

1. Liu C, Qin H, Mather PT (2007) J Mater Chem 17:1543–1558
2. Dietsch B, Tong T (2007) J Adv Mater 39:3–12
3. Havens E, Snyder E, Tong T (2005) Proc SPIE 5762:48–54
4. Ratna D, Karger-Kocsis J (2008) J Mater Sci 43:254–269
5. Gunes IS, Jana SC (2008) J Nanosci Nanotechnol 8:1616–1637
6. Mather PT, Luo XF, Rousseau IA (2009) Annu Rev Mater Res 39:445–471
7. Lendlein A (2010) Shape-memory polymers. Springer, Berlin
8. Toensmeier PA (2005) Plast Eng 61:10–11
9. Hidber PC, Nealey PF, Helbig W, Whitesides GM (1996) Langmuir 12:5209–5215
10. Liu N, Huang WM, Phee SJ, Tong TH (2008) Smart Mater Struct 17:057001
11. Liu XC, Chakraborty A, Luo C (2010) J Micromech Microeng 20:095025
12. Wang Z, Hansen C, Ge Q, Maruf SH, Ahn DU, Qi HJ, Ding YF (2011) Adv Mater 23:3669–3673
13. Zhao Y, Huang WM, Fu YQ (2011) J Micromech Microeng 21:067007
14. Baer G, Wilson TS, Matthews DL, Maitland DJ (2007) J Appl Polym Sci 103:3882–3892
15. Sokolowski W, Metcalfe A, Hayashi S, Yahia L, Raymond J (2007) Biomed Mater 2:S23–S27
16. Yakacki CM, Shandas R, Safranski D, Ortega AM, Sassaman K, Gall K (2008) Adv Funct Mater 18:2428–2435
17. Sun L, Huang WM (2010) Mater Des 31:2684–2689
18. Wischke C, Lendlein A (2010) Pharm Res 27:527–529
19. Lake MS, Campbell D (2004) IEEE Aerosp Conf Proc 2745–2756
20. Sokolowski WM, Tan SC (2007) J Spacecraft Rockets 44:750–754
21. Chiodo JD, Harrison DJ, Billett EH (2001) P I Mech Eng B-J Eng 215:733–741
22. Hussein H, Harrison D (2008) Int J Prod Dev 6:431–449
23. Sun L, Huang WM, Ding Z, Zhao Y, Wang CC, Purnawali H, Tang C (2012) Mater Des 33:577–640
24. Aschwanden M, Stemmer A (2006) Opt Lett 31:2610–2612
25. Haertling GH (1999) J Am Ceram Soc 82:797–818
26. Otsuka K, Wayman CM (1998) Shape memory materials. Cambridge University Press, New York
27. Miyazaki S, Fu YQ, Huang WM (2009) Thin film shape memory alloys: fundamentals and device applications. Cambridge University Press, New York
28. Leng J, Du S (2010) In: CRC Press/Taylor & Francis, Boca Raton
29. Huang WM, Yang B, Fu YQ (2011) Polyurethane shape memory polymers. CRC Press, USA
30. Xie T, Page KA, Eastman SA (2011) Adv Funct Mater 21:2057–2066
31. Amirian M, Chakoli AN, Sui JH, Cai W (2012) J Polym Res 19
32. Liu GQ, He WC, Peng YX, Xia HS (2011) J Polym Res 18:2109–2117
33. Schmidt C, Chowdhury AMS, Neuking K, Eggeler G (2011) J Polym Res 18:1807–1812
34. Zhao Y, Wang CC, Huang WM, Purnawali H (1913) Appl Phys Lett 99(2011):131911–131913
35. Beloshenko VA, Varyukhin VN, Voznyak YV (2005) Russ Chem Rev 74:265–283
36. Chaunier L, Lourdin D (2009) Starch-Starke 61:116–118
37. Mendez J, Annamalai PK, Eichhorn SJ, Rusli R, Rowan SJ, Foster EJ, Weder C (2011) Macromolecules 44:6827–6835
38. Chang BTA, Li JCM (1980) J Mater Sci 15:1364–1370
39. Chang BTA, Li JCM (1981) J Mater Sci 16:889–899
40. Dismore PF, Statton WO (1964) J Polym Sci B Pol Lett 2:1113–1116
41. Dumbleton JH (1969) J Polym Sci A2(7):667–674
42. Statton WO, Koenig JL, Hannon M (1970) J Appl Phys 41:4290–4295
43. Wilson MPW (1974) Polym 15:277–282
44. Crystal RG, Hansen D (1967) J Appl Phys 38:3103–3108
45. Ito E, Horie T, Kobayashi Y (1978) J Appl Polym Sci 22:3193–3201
46. Wing G, Pasricha A, Tuttle M, Kumar V (1995) Polym Eng Sci 35:673–679
47. Yang FQ, Li JCM (1997) J Mater Res 12:2809–2814
48. Yang FQ, Zhang SL, Li JCM (1997) J Electron Mater 26:859–862
49. Kung TM, Li JCM (1987) J Mater Sci 22:3620–3630
50. Quinson R, Perez J, Germain Y, Murraciole JM (1995) Polym 36:743–752
51. Quinson R, Perez J, Rink M, Pavan A (1996) J Mater Sci 31:4387–4394
52. Xie T (2011) Polym 52:4985–5000
53. Maitland DJ, Metzger MF, Schumann D, Lee A, Wilson TS (2002) Laser Surg Med 30:1–11
54. Koerner H, Price G, Pearce NA, Alexander M, Vaia RA (2004) Nat Mater 3:115–120
55. Cho JW, Kim JW, Jung YC, Goo NS (2005) Macromol Rapid Comm 26:412–416
56. Yang B, Huang WM, Li C, Chor JH (2005) Eur Polym J 41:1123–1128
57. Schmidt AM (2006) Macromol Rapid Comm 27:1168–1172
58. Meng QH, Hu JL, Yeung L (2007) Smart Mater Struct 16:830–836
59. Leng JS, Huang WM, Lan X, Liu YJ, Du SY (2008) Appl Phys Lett 92:204101

60. Yakacki CM, Satarkar NS, Gall K, Likos R, Hilt JZ (2009) J Appl Polym Sci 112:3166–3176
61. Gunes IS, Jimenez GA, Jana SC (2009) Carbon 47:981–997
62. Jiang HY, Kelch S, Lendlein A (2006) Adv Mater 18:1471–1475
63. Kumpfer JR, Rowan SJ (2011) J Am Chem Soc 133:12866–12874
64. Fomina N, McFearin CL, Sermsakdi M, Morachis JM, Almutairi A (2011) Macromolecules 44:8590–8597
65. Huang W (2002) Mater Des 23:11–19
66. Huang WM, Ding Z, Wang CC, Wei J, Zhao Y, Purnawali H (2010) Mater Today 13:54–61
67. Fu CC, Grimes A, Long M, Ferri CGL, Rich BD, Ghosh S, Ghosh S, Lee LP, Gopinathan A, Khine M (2009) Adv Mater 21:4472–4476
68. Sun L, Zhao Y, Huang WM, Tong TH (2009) Surf Rev Lett 16:929–933
69. Huang WM, Liu N, Lan X, Lin JQ, Pan JH, Leng JS, Phee SJ, Fan H, Liu YJ, Tong TH (2009) Mater Sci Forum 614:243–248
70. Li JH, Viveros JA, Wrue MH, Anthamatten M (2007) Adv Mater 19:2851–2855
71. Kushner AM, Vossler JD, Williams GA, Guan ZB (2009) J Am Chem Soc 131:8766–8768
72. Jeffrey GA (1997) An introduction to hydrogen bonding. Oxford University Press, New York
73. Page KA, Cable KM, Moore RB (2005) Macromolecules 38:6472–6484
74. Li FK, Zhu W, Zhang X, Zhao CT, Xu M (1999) J Appl Polym Sci 71:1063–1070
75. Hayashi S (1990) Technical report on preliminary investigation of shape memory polymers, Nagoya research and development center. Mitsubishi Heavy Industries Inc., Japan
76. Ping P, Wang WS, Chen XS, Jing XB (2005) Biomacromolecules 6:587–592
77. Kim BK, Lee SY, Xu M (1996) Polym 37:5781–5793
78. Li FK, Zhang X, Hou JN, Xu M, Luo XL, Ma DZ, Kim BK (1997) J Appl Polym Sci 64:1511–1516
79. Wang WS, Ping P, Chen XS, Jing XB (2006) Eur Polym J 42:1240–1249
80. Xu JW, Shi WF, Pang WM (2006) Polym 47:457–465
81. Hu J (2007) Shape memory polymers and textiles. Woodhead Publishing Limited, Cambridge
82. Chung YC, Choi JH, Chun BC (2008) J Mater Sci 43:6366–6373
83. Park JS, Chung YC, Do Lee S, Cho JW, Chun BC (2008) Fiber Polym 9:661–666
84. Jung DH, Jeong HM, Kim BK (2010) J Mater Chem 20:3458–3466
85. Behl M, Ridder U, Feng Y, Kelch S, Lendlein A (2009) Soft Matter 5:676–684
86. Jeong HM, Song JH, Lee SY, Kim BK (2001) J Mater Sci 36:5457–5463
87. Weiss RA, Izzo E, Mandelbaum S (2008) Macromolecules 41:2978–2980
88. Luo X, Mather PT (2009) Macromolecules 42:7251–7253
89. Guan Y, Cao Y, Peng Y, Xu J, Chen ASC (2001) Chem Commun 1694–1695
90. Fan K, Huang WM, Wang CC, Ding Z, Zhao Y, Purnawali H, Liew KC, Zheng LX (2011) Express Polym Lett 5:409–416
91. Sun L, Huang WM, Wang CC, Zhao Y, Ding Z, Purnawali H (2011) J Polym Sci A Polym Chem 49:3574–3581
92. Liu N, Huang WM, Phee SJ, Fan H, Chew KL (2007) Smart Mater Struct 16:N47–N50
93. Liu N, Xie Q, Huang WM, Phee SJ, Guo NQ (2008) J Micromech Microeng 18:027001
94. O'Brien B, Carroll W (2009) Acta Biomater 5:945–958
95. H. Paakinaho, H. Heino, P. Tormala, T. Allinniemi, in
96. Lendlein A, Langer R (2002) Science 296:1673–1676
97. Min CC, Cui WJ, Bei JZ, Wang SG (2005) Polym Advan Technol 16:608–615
98. Kelch S, Steuer S, Schmidt AM, Lendlein A (2007) Biomacromolecules 8:1018–1027
99. Wischke C, Neffe AT, Steuer S, Lendlein A (2009) J Control Release 138:243–250
100. Wischke C, Neffe AT, Lendlein A (2010) Controlled drug release from biodegradable shape-memory polymers. In: Lendlein A (ed) Advances in polymer science: shape-memory polymers. Springer, Heidelberg, pp 177–205
101. Zhang SF, Feng YK, Zhang L, Guo JT, Xu YS (2010) J Appl Polym Sci 116:861–867
102. Liu N, Huang WM, Phee SJ (2007) Surf Rev Lett 14:1187–1190
103. Rodriguez ED, Luo X, Mather PT (2011) ACS Appl Mater Interfaces 3:152–161
104. Yang B, Huang WM, Li C, Lee CM, Li L (2004) Smart Mater Struct 13:191–195
105. Jung YC, So HH, Cho JW (2006) J Macromol Sci B 45:453–461
106. Willett JL (2008) Macromol Chem Physic 209:764–772
107. Chen SJ, Hu JL, Yuen CWM, Chan LK (2009) Polym 50:4424–4428
108. Du HY, Zhang JH (2010) Soft Matter 6:3370–3376
109. Yang B, Huang WM, Li C, Li L (2006) Polym 47:1348–1356
110. Huang WM, Yang B, Zhao Y, Ding Z (2010) J Mater Chem 20:3367–3381
111. Huang WM, Yang B, An L, Li C, Chan YS (2005) Appl Phys Lett 86:114105
112. Zhao XM, Xia YN, Schueller OJA, Qin D, Whitesides GM (1998) Sensor Actuat A-Phys 65:209–217
113. Grimes A, Breslauer DN, Long M, Pegan J, Lee LP, Khine M (2008) Lab Chip 8:170–172
114. Lv HB, Leng JS, Liu YJ, Du SY (2008) Adv Eng Mater 10:592–595
115. Harmon JP, Lee S, Li JCM (1987) J Polym Sci A Polym Chem 25:3215–3229
116. Harmon JP, Lee S, Li JCM (1988) Polym 29:1221–1226
117. Petrovic ZS, Javni I, Divjakovic V (1998) J Polym Sci B Pol Phys 36:221–235
118. Chaterji S, Kwon IK, Park K (2007) Prog Polym Sci 32:1083–1122
119. Jagur-Grodzinski J (2010) Polym Advan Technol 21:27–47
120. Aw MS, Simovic S, Addai-Mensah J, Losic D (2011) J Mater Chem 21:7082–7089
121. Xing SY, Guan Y, Zhang YJ (2011) Macromolecules 44:4479–4486
122. Zha LS, Banik B, Alexis F (2011) Soft Matter 7:5908–5916
123. Qiu Y, Park K (2001) Adv Drug Deliver Rev 53:321–339
124. Kim YB, Chung CW, Kim HW, Rhee YH (2005) Macromol Rapid Comm 26:1070–1074
125. Deka H, Karak N, Kalita RD, Buragohain AK (2010) Carbon 48:2013–2022
126. Kamiya N, Shiotari Y, Tokunaga M, Matsunaga H, Yamanouchi H, Nakano K, Goto M (2009) Chem Commun 5287–5289
127. Cosgrove L, McGeechan PL, Robson GD, Handley PS (2007) Appl Environ Microb 73:5817–5824
128. Ulijn RV (2006) J Mater Chem 16:2217–2225
129. Huang WM, Yang B, Li C, Chan YS, An L (2010) Appl Phys Lett 97:056102
130. Huang WM, Lee CW, Teo HP (2006) J Intel Mat Syst Str 17:753–760
131. Tobushi H, Okumura K, Endo M, Hayashi S (2001) J Intel Mat Syst Str 12:283–287
132. Tobushi H, Matsui R, Hayashi S, Shimada D (2004) Smart Mater Struct 13:881–887
133. Tey SJ, Huang WM, Sokolowski WM (2001) Smart Mater Struct 10:321–325

134. Zhang CS, Ni QQ (2007) Compos Struct 78:153–161
135. Voit W, Ware T, Dasari RR, Smith P, Danz L, Simon D, Barlow S, Marder SR, Gall K (2010) Adv Funct Mater 20:162–171
136. Zhang YM, Wang QH, Wang C, Wang TM (2011) J Mater Chem 21:9073–9078
137. Yakacki CM, Willis S, Luders C, Gall K (2008) Adv Eng Mater 10:112–119
138. Feldkamp DM, Rousseau IA (2010) Macromol Mater Eng 295:726–734
139. Kratz K, Madbouly SA, Wagermaier W, Lendlein A (2011) Adv Mater 23:4058–4062
140. Purnawali H, Xu WW, Zhao Y, Ding Z, Wang CC, Huang WM (2012) Smart Mater Struct 21:075006
141. Zhang H, Wang HT, Zhong W, Du QG (2009) Polym 50:1596–1601
142. Levoy M, Ng R, Adams A, Footer M, Horowitz M (2006) ACM Trans Graphics 25:924–934
143. Kim JJ, Chae S, Jeong KH (2010) Opt Lett 35:823–825
144. Lin GL, Cheng CC (2008) IAENG Int J Comput Sci 35:242–248
145. Liu C, Mather PT (2002) J Appl Med Polym 6:47–52
146. Xie T, Rousseau IA (2009) Polym 50:1852–1856
147. Bhattacharya K, James RD (2005) Science 307:53–54
148. DiOrio AM, Luo XF, Lee KM, Mather PT (2011) Soft Matter 7:68–74
149. Behl M, Bellin I, Kelch S, Wagermaier W, Lendlein A (2009) Adv Funct Mater 19:102–108
150. Bellin I, Kelch S, Langer R, Lendlein A, Natl P (2006) Acad Sci USA 103:18043–18047
151. Bellin I, Kelch S, Lendlein A (2007) J Mater Chem 17:2885–2891
152. Luo X, Mather PT (2010) Adv Funct Mater 20:2649–2656
153. Pretsch T (2010) Smart Mater Struct 19:015006
154. He ZW, Satarkar N, Xie T, Cheng YT, Hilt JZ (2011) Adv Mater 23:3192–3196
155. Xie T, Xiao XC, Cheng YT (2009) Macromol Rapid Comm 30:1823–1827
156. Bae CY, Park JH, Kim EY, Kang YS, Kim BK (2011) J Mater Chem 21:11288–11295
157. Xie T (2010) Nature 464:267–270
158. Sun L, Huang WM (2010) Soft Matter 6:4403–4406
159. Huang WM, Song CL, Fu YQ, Wang CC, Zhao Y, Purnawali H, Lu HB, Tang C, Ding Z, Zhang JL(in press) Adv Drug Delivery Rev
160. Airoldi G, Besseghini S, Riva G (1993) Il Nuovo Cimento D 15:365–374
161. Madangopal K, Banerjee S, Lele S (1994) Acta Metall Mater 42:1875–1885
162. Liu N, Huang WM (2006) Scripta Mater 55:493–495
163. Liu N, Huang WM (2006) Trans Nonferr Metal Soc 16:S37–S41
164. Sun L, Huang WM, Cheah JY (2010) Smart Mater Struct 19:055005
165. Miaudet P, Derre A, Maugey M, Zakri C, Piccione PM, Inoubli R, Poulin P (2007) Science 318:1294–1296
166. Hu ZB, Zhang XM, Li Y (1995) Science 269:525–527
167. Osada Y, Gong JP (1998) Adv Mater 10:827–837
168. Ju HK, Kim SY, Lee YM (2001) Polym 42:6851–6857
169. Roy D, Cambre JN, Sumerlin BS (2010) Prog Polym Sci 35:278–301
170. Li YL, Maciel D, Tomas H, Rodrigues J, Ma H, Shi XY (2011) Soft Matter 7:6231–6238
171. Wang WB, Xu JX, Wang AQ (2011) Express Polym Lett 5:385–400
172. Sun L, Huang WM (2009) Adv Compos Mater 18:95–103
173. Osada Y, Matsuda A (1995) Nature 376:219
174. Mitsumata T, Gong JP, Osada Y (2001) Polym Advan Technol 12:136–150
175. Wang X, Hong W (2011) Soft Matter 7:8576–8581
176. Webber RE, Creton C, Brown HR, Gong JP (2007) Macromolecules 40:2919–2927
177. Mano JF (2008) Adv Eng Mater 10:515–527
178. Serrano MC, Carbajal L, Ameer GA (2011) Adv Mater 23:2211–2215
179. Di Palma JA, Cleveland MV, McGowan J, Herrera JL (2007) Am J Gastroenterol 102:1964–1971
180. van Vlerken LE, Vyas TK, Amiji MM (2007) Pharm Res 24:1405–1414
181. Mero A, Schiavon O, Pasut G, Veronese FM, Emilitri E, Ferruti P (2009) J Bioact Compat Pol 24:220–234
182. Chaunier L, Véchambre C, Lourdin D (2012) Food Res Inter 47:194–196
183. Tobushi H, Hayashi S, Hoshio K, Ejiri Y (2008) Sci Technol Adv Mat 9:015009
184. Lorenzo V, Diaz-Lantada A, Lafont P, Lorenzo-Yustos H, Fonseca C, Acosta J (2009) Mater Des 30:2431–2434
185. Pretsch T, Müller WW (2010) Polym Degrad Stabil 95:880–888
186. Pretsch T, Jakob I, Muller W (2009) Polym Degrad Stabil 94:61–73
187. Pretsch T (2010) Polymers 2:120–158
188. Pretsch T (2010) Polym Degrad Stabil 95:2515–2524
189. Xu T, Li GQ (2011) Mater Sci Eng A-Struct 528:7444–7450
190. Kunzelman J, Chung T, Mather PT, Weder C (2008) J Mater Chem 18:1082–1086
191. Dumortier G, Grossiord JL, Agnely F, Chaumeil JC (2006) Pharm Res 23:2709–2728
192. Wang CC, Huang WM, Zhao Y, Ding Z, Purnawali H (2012) Comp Sci Tech 72:1178–1182
193. Xiao X, Xie T, Cheng Y-T (2010) J Mater Chem 20:3508–3514